ERDC/EL TR-08-40

US Army Corps
of Engineers®
Engineer Research and
Development Center

*Environmental Quality and Installations Program*

# UXO Characterization: Comparing Cued Surveying to Standard Detection and Discrimination Approaches

Report 9 of 9
Former Lowry Bombing and Gunnery Range; Comparison of UXO Characterization Performance Using Area and Cued-interrogation Survey Modes

Stephen D. Billings, Leonard R. Pasion, Kevin Kingdon,
Sean Walker, and Jon Jacobson

September 2008



Environmental Laboratory

Environmental Quality and Installations Program

ERDC/EL TR-08-40
September 2008

# UXO Characterization: Comparing Cued Surveying to Standard Detection and Discrimination Approaches

Report 9 of 9
Former Lowry Bombing and Gunnery Range; Comparison of UXO Characterization Performance Using Area and Cued-interrogation Survey Modes

Stephen D. Billings, Leonard R. Pasion, Kevin Kingdon, Sean Walker, and Jon Jacobson

*Sky Research, Inc.*
*445 Dead Indian Memorial Rd.*
*Ashland, OR 97520-9706*

Report 9 of 9



Prepared for Headquarters, U.S. Army Corps of Engineers
Washington, DC 20314-1000

Monitored by Environmental Laboratory
U.S. Army Engineer Research and Development Center
3909 Halls Ferry Road, Vicksburg, MS 39180-6199

**Abstract:** This report describes the collection, processing, interpretation, and analysis of Geonics EM-63 and Geophex GEM-3 data collected in a cued-interrogation mode at the FLBGR and compares the discrimination potential of data collected in discrimination versus cued-interrogation modes. The higher quality, better positioning, and denser coverage of the EM-63 cued-interrogation data (compared to discrimination mode data) result in a significant improvement in the discrimination potential of the system. For the GEM-3 data, which were collected in cued-interrogation mode, the amplitude and time constants of the four-parameter model of Miller et al. appeared to provide good discrimination potential. When deployed in a cued-interrogation mode, the GEM-3 appears to be capable of distinguishing 37-mm projectiles from 20-mm projectiles AND of distinguishing 20-mm projectiles from 50-caliber bullets.

# Contents

# Figures and Tables

## Figures

## Tables

# Preface

This report was prepared as part of the Congressional Interest Environmental Quality and Installations Program, Unexploded Ordnance (UXO) Focus Area, Contract No. W912HZ-04-C-0039, Purchase Request No. W81EWF-418-0425, titled, "UXO Characterization: Comparison of Cued Surveying to Standard Detection and Standard Discrimination Approaches." Research was conducted by Sky Research, Inc., for the Environmental Laboratory (EL), U.S. Army Engineer Research and Development Center (ERDC), Vicksburg, MS. The following Sky Research personnel contributed to this report:

- Dr. Stephen D. Billings was the project Principal Investigator and oversaw data collection and analysis of field data, and produced the report for this segment of the project;
- Dr. Leonard R. Pasion conducted quality control of the parametric inversions;
- Kevin Kingdon, Sean Walker, and Jon Jacobson assisted with the data collection and processing of the data.
- Joy Rogalla was the copy editor for this report;
- Daniel Connoly and Casey McDonald assisted with the GEM-3 and EM-63 data collection efforts.

The following Tetra-Tech EMI personnel contributed to this report:

- Kevin Kobel was the UXO Technician responsible for collection of the ground-truth information.

The work conducted at the Former Lowry Bombing and Gunnery Range was co-sponsored under ESTCP Project MM-0504. In addition, the USACE-Omaha district provided logistical support and supplied EOD escorts for both the geophysical surveys and the intrusive investigations. The authors would especially like to thank Jerry Hodgson from USACE-Omaha, who supported this project throughout its duration.

This project was performed under the general supervision of Dr. M. John Cullinane, Jr., Technical Director, Military Environmental Engineering and Sciences, EL and Mr. John H. Ballard, Office of Technical Director

and UXO Focus Area Manager, EL. Reviews were provided by Ballard and Dr. Dwain Butler, Alion Science and Technology Corporation. Dr. Beth Fleming was Director, EL.

COL Gary E. Johnston was Commander and Executive Director of ERDC. Dr. James R. Houston was Director.

# Unit Conversion Factors

| Multiply | By | To Obtain |
|---|---|---|
| acres | 4,046.873 | square meters |
| miles (U.S. statute) | 1,609.347 | meters |

# Acronyms

| | |
|---|---|
| cm | centimeters |
| DoD | Department of Defense |
| DSB | Defense Science Board |
| EMI | Electromagnetic Induction |
| EOD | Explosives and Ordnance Disposal |
| ERDC | Engineer Research and Development Center |
| ESTCP | Environmental Security Technology Certification Program |
| FLBGR | Former Lowry Bombing and Gunnery Range |
| GPR | Ground Penetrating Radar |
| HE | High Explosive |
| IMU | Inertial Motion Unit |
| m | meter(s) |
| MEC | Munitions and Explosives of Concern |
| mm | millimeter(s) |
| ms | millisecond(s) |
| mV | millivolt(s) |
| RF | Range Fan |
| RR | Rocket Range |
| RTS | Robotic Total Station |
| SNR | Signal-to-Noise Ratio |
| SVM | Support Vector Machine |
| UTM | Universal Transverse Mercator |
| UXO | Unexploded Ordnance |
| USACE | U.S. Army Corps of Engineers |

# General Introduction

The clearance of military facilities in the United States contaminated with unexploded ordnance (UXO) is one of the most significant environmental concerns facing the Department of Defense (DoD). A 2003 report by the Defense Science Board (DSB) on the topic estimated costs of remediation in the tens of billions of dollars. The DSB recognized that developing effective discrimination strategies to distinguish UXO from non-hazardous material is one essential technology area where the greatest cost saving to the DoD can be achieved.

The objective of project W912HZ-04-C-0039 "UXO Characterization: Comparison of Cued Surveying to Standard Detection and Standard Discrimination Approaches," was to research, develop, optimize, and evaluate the efficiencies of different modes of UXO characterization and remediation as a function of the density of UXO and associated clutter. Survey modes investigated in the research include:

1. Standard detection survey: All selected anomalies are excavated;
2. Advanced discrimination survey: Data collected in proximity to each identified anomaly are inverted for physics-based parameters and statistical or analytical classifiers are used to rank anomalies, from which a portion of the higher ranked anomalies are excavated;
3. Cued-survey mode: Each selected anomaly is revisited with an interrogation platform, high-quality data are collected and analyzed, and a decision is made as to whether to excavate the item, or leave it in the ground.

Specific technical objectives of the research were to:

- Determine the feasibility and effectiveness of various interrogation approaches based on the cued-survey approach;
- Determine the feasibility and effectiveness of various interrogation sensors including magnetics, ground penetrating radar (GPR), and electromagnetic induction (EMI), and evaluate combinations of these sensors;
- Develop and evaluate the most promising interrogation platform designs;

- Develop optimal processing and inversion approaches for cued-interrogation platform datasets;
- Evaluate the data requirements to execute accurate target parameterization and assess the technical issues of meeting these requirements using detection and interrogation survey techniques;
- Determine which survey mode is most effective as a function of geological interference and UXO/clutter density;
- Investigate the feasibility and effectiveness of using detailed test-stand measurements on UXO and clutter to assist in the design of interrogation algorithms used in the cued-search mode.

The main areas of research involved in these coordinated activities include:

- Sensor phenomenology, including GPR, EMI, and magnetometry;
- Data Collection Systems; platforms, field survey systems, field interrogation systems;
- Parameter estimation techniques; inversion techniques (single, cooperative, joint), forward-model parameterizations, processing strategies; and
- Classification methods; thresholding, statistical models, information systems.

This report "UXO Characterization: Comparing Cued Surveying to Standard Detection and Discrimination Approaches: Report 9 of 9 – Former Lowry Bombing and Gunnery Range: Comparison of UXO Characterization Performance Using Area and Cued-interrogation Survey Modes" is one of a series of nine reports written as part of W912HZ-04-C-0039:

1. UXO Characterization: Comparing Cued Surveying to Standard Detection and Discrimination Approaches: Report 1 of 9 – Summary Report;
2. UXO Characterization: Comparing Cued Surveying to Standard Detection and Discrimination Approaches: Report 2 of 9 – Ground Penetrating Radar for Unexploded Ordnance Characterization; Fundamentals;
3. UXO Characterization: Comparing Cued Surveying to Standard Detection and Discrimination Approaches: Report 3 of 9 – Test Stand Magnetic and Electromagnetic Measurements of Unexploded Ordnance;

4. UXO Characterization: Comparing Cued Surveying to Standard Detection and Discrimination Approaches: Report 4 of 9 – UXO Characterization Using Magnetic, Electromagnetic, and Ground Penetrating Radar Measurements at the Sky Research Test Plot;
5. UXO Characterization: Comparing Cued Surveying to Standard Detection and Discrimination Approaches: Report 5 of 9 – Optimized Data Collection Platforms and Deployment Modes for Unexploded Ordnance Characterization;
6. UXO Characterization: Comparing Cued Surveying to Standard Detection and Discrimination Approaches: Report 6 of 9 – Advanced Electromagnetic and Magnetic Methods for Discrimination of Unexploded Ordnance;
7. UXO Characterization: Comparing Cued Surveying to Standard Detection and Discrimination Approaches: Report 7 of 9 – Marine Corps Base Camp Lejeune: UXO Characterization Using Ground Penetrating Radar;
8. UXO Characterization: Comparing Cued Surveying to Standard Detection and Discrimination Approaches: Report 8 of 9 – Marine Corps Base Camp Lejeune: UXO Characterization Using Magnetic and Electromagnetic Data;
9. UXO Characterization: Comparing Cued Surveying to Standard Detection and Discrimination Approaches: Report 9 of 9 – Former Lowry Bombing and Gunnery Range: Comparison of UXO Characterization Performance Using Area and Cued-interrogation Survey Modes.

# 1 Introduction

## 1.1. Background

The Former Lowry Bombing and Gunnery Range (FLBGR) was the principal site used to compare discrimination and cued-interrogation mode datasets under this project. Two sites were selected at FLBGR. The first was the 20-mm Range Fan (RF) where the objective was to distinguish hazardous 37-mm projectiles from less hazardous and ubiquitous 20-mm projectiles and 50-caliber bullets. This represented a difficult *small-object* discrimination scenario. The second site was the Rocket Range (RR), where there was the potential to encounter a mixed range of ordnance including bombs and projectiles.

In conjunction with the Environmental Security Technology Certification Program (ESTCP) project MM-0504, discrimination mode Geonics EM-61, Geonics EM-63, and Geometrics cesium vapor magnetics data were collected over 8 acres on the RR and 2 acres on the 20-mm RF. The collection, processing, validation, interpretation, and retrospective analysis of those data are presented in a demonstration report prepared under the MM-0504 project (Billings et al. 2007). The executive summary of that report is reproduced below.

This report describes the collection of the EM-63 and GEM-3 cued-interrogation data at the 20-mm RF and the RR. Feature vectors derived from the EM-63 cued-interrogation data are compared to those obtained from the discrimination mode data. Lastly, the GEM-3 cued-interrogation data are analyzed and the discrimination potential of those data is determined.

The primary objective of this report is to quantify the improvement in discrimination potential that can be achieved using cued-interrogation data. The report does not include a cost-benefit analysis of discrimination versus cued-interrogation modes of surveying. This is because the most *efficient and effective* survey mode for a given site will depend on a multitude of site-specific factors. These include the type and diversity of UXO and clutter encountered, the risk and cost of excavating each anomaly, and the vegetation, terrain, cultural features, and geology of the site.

## 1.2. Executive Summary from ESTCP MM-0504 Demonstration Report

The executive summary of the Environmental Security Technology Certification Program (ESTCP) project MM-0504 demonstration report (Billings et al. 2007) is reproduced below.

> This demonstration described in this report was conducted under project ESTCP MM-0504 "Practical Discrimination Strategies for Application to Live Sites." This project is attempting to demonstrate the application of feature extraction and statistical classification to the problem of UXO discrimination. The demonstration utilized Geonics EM-61 MK-II towed array and Geonics EM-63 cart-based data collected at two sites on the Former Lowry Bombing and Gunnery Range, Colorado. The demonstrations were conducted with the support of the USACE-Omaha and USACE-ERDC. The objectives of the Rocket Range surveys (8 acres) were the discrimination of a mixed range of projectiles with minimum diameter of 37 mm from shrapnel, junk, 20-mm projectiles, and small arms. The 20-mm Range Fan survey (2 acres) presented a small-item discrimination scenario where the objective was to discriminate 37-mm projectiles from ubiquitous 20-mm projectiles and 50-caliber bullets. Both EM systems trialed were positioned by a Leica TPS 1206 Robotic Total Station, with orientation information provided by a Crossbow AHRS 400 Inertial Motion Unit. Data processing, feature extraction, and statistical classification were all conducted within the University of British Columbia's UXOLab software package. For the EM-61, three-dipole instantaneous amplitude models were fit to the available four time channels, while for the EM-63, three-dipole Pasion-Oldenburg models were recovered from the 26 time-channel data. Parameters of the dipole model were used to guide a statistical classification. Canonical and visual analysis of feature vectors extracted form the test-plot data indicated that discrimination could best proceed using a combination of a size- and a goodness of fit-based feature vector. A Support Vector Machine classifier was then implemented based on those feature vectors and using the available training data.

Two phases of digging and training were conducted at the 20-mm RF, and three phases at the Rocket Range. At the Rocket Range, 29 MK-23 practice bombs were recovered, with only one other UXO encountered (a 2.5-in. rocket warhead). At the 20-mm Range Fan, thirty-eight 37-mm projectiles (most of them emplaced) were recovered, as were a large number of 20-mm projectiles and 50-caliber bullets. For both sites, and for both instruments, the SVM classifier outperformed a ranking based on amplitude alone. In each case, the last detected UXO was ranked quite high by the SVM classifier and digging to that point would have resulted in a 60- to 90-percent reduction in the number of false alarms. This operating point is of course unknown prior to digging. Using a stop-digging criteria of f = 0 (mid-way between UXO and clutter class support planes) was too aggressive and more excavations were typically required for full recovery of detected UXO. Both the amplitude and SVM methods performed quite poorly on two deep (40 cm) emplaced 37-mm projectiles at the 20-mm Range Fan, exposing a potential weakness of the goodness of fit metric. Retrospective analysis revealed that thresholding on the size of the polarization tensor alone would have yielded good discrimination performance.

At the 20-mm Range Fan it was found that 50-caliber bullets caused more false alarms than 20-mm projectiles, even though they are significantly smaller. Retrospective analysis revealed that this was caused by a lower SNR[1] on the 50-caliber bullets. There was insufficient SNR to constrain the depth of the item and inversion solutions tended to be pushed deep due to either flat-objective functions or the presence of multiple locally optimal solutions. Consequently, size estimates of 50-caliber bullets obtained from the amplitude of the polarization tensor varied across four orders of magnitude and tended to be overestimated. For the larger 20- and 37-mm projectiles, size estimates varied by around two-orders of magnitude, but there was less overlap between the two classes. Relatively poor depth performance on

[1] Positioning error and sparse data coverage also likely contributed to the inability to constrain size.

shallow, high SNR MK-23 practice bombs at the Rocket Range indicates that positional errors (and potentially unmodeled dipole components) also cause uncertainty in the object depth (and hence in the object size). It is concluded that depth and size are poorly constrained when estimated from single component sensor data obtained with currently available positional precision. However, size estimates may still provide useful information to prioritize digging order.

During the demonstration, feature vectors derived from the time-decay properties of the polarization tensor were not used to aid discrimination performance of either instrument. The noise floor decays as $1/t^{0.5}$, while signal falls off more rapidly. This means that the accuracy of time-decay parameters extracted from low SNR anomalies is generally limited. However, retrospective analysis revealed that time-decay properties of the principal polarization tensor could have been used to distinguish MK-23 practice bombs from other items on the Rocket Range (for both instruments). On the 20-mm Range Fan, the time range of the EM-63 is long enough that the slower decay rate of the 37-mm projectiles could have been distinguished from 20-mm projectiles. In contrast, the EM-61 did not sample late enough in time to aid discrimination.

EM-61 and EM-63 discrimination results when using size-based feature vectors were comparable on both sites. Speed of survey, ease of use, and reliability make the EM-61 more suited for this mode of discrimination. The techniques could be immediately transitioned into production field use on the 20-mm Range Fan. At the Rocket Range, additional testing to verify performance against more munitions types would need to be conducted. The EM-63 is better suited for a cued-interrogation mode, where it has the potential to constrain the time-decay properties of the polarization over a wider time range.

# 2 Surveys Conducted at FLBGR

## 2.1. Test site history/characteristics

FLBGR is located approximately 20 miles southeast of Denver, Colorado, in Arapahoe County. Although the area immediately west of the former bombing range is extensively developed, the site is still primarily grazing land. Evidence of Department of Defense (DoD) use of the bombing range remains at every known range. The gunnery ranges and small arms ranges still contain empty cartridges and projectiles.

FLBGR was originally part of Buckley Field, which consisted of the airfield and bombing and gunnery range and covered 65,547 acres. The status of the various parcels of land that comprised Buckley Field changed several times since the land was acquired by the City of Denver beginning in 1937. The airfield and bombing range were used by the Army during World War II. After the war, the airfield became a Naval Air Station and the bombing range came under the custody of Lowry Air Force Base. The bombing range was renamed the Lowry Bombing and Gunnery Range. The bombing range was excessed beginning in 1960.

In 2005, 45 acres on the RR and 6 acres on the 20-mm RF were surveyed with the Sky Research EM-61 towed array (Figure 1). These areas were specifically identified by USACE-Omaha as priority areas that are currently being cleared (or will be cleared in the near future). The sites are also representative of the terrain, vegetation, and munitions at the site.

The RR was used for bombing practice with sand-filled practice bombs and high explosive (HE) bombs, rocket practice, and gunnery training. Expected munitions and explosives of concern (MEC) in this area include practice bomb debris, HE bomb fragments, 50-caliber ammunition, and 20-mm projectiles and practice rockets.

The 20-mm RF was used for air-to-ground target practice for fixed-wing aircraft firing 50-caliber projectiles, and 20- and 37-mm projectiles.

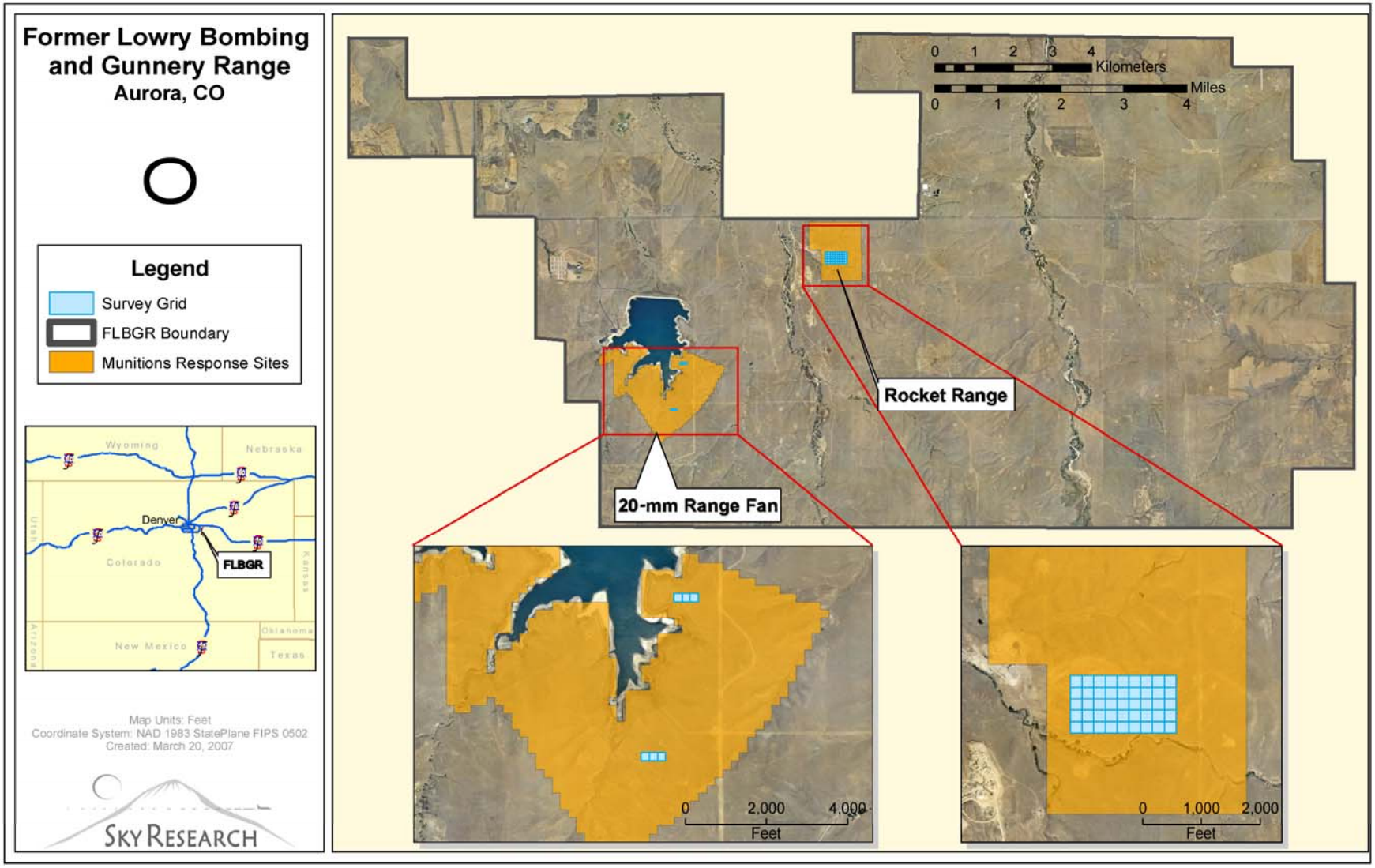


Figure 1. Locations of the Rocket Range and 20-mm Range Fan sites at FLBGR.

Within the demonstration areas, there is little variation in terrain and vegetation. At both sites the vegetation is a mixture of grasses and Yucca plants. These are dense, low-lying (< 1 m) plants that caused some survey difficulties to the EM-63 cart in particular.

## 2.2. Pre-demonstration testing and analysis

In September/October 2005, the FLBGR test grid (Figure 2), 45 acres on the RR (Figure 3), and 6 acres on the 20-mm Range Fan (3 acres are shown in Figure 4) were surveyed with the EM-61 towed array with robotic total station (RTS) and inertial motion unit (IMU). These towed array data were used for the EM-61 inversions conducted as part of this demonstration.

Targets were selected with a 10-millivolt (mV) threshold on time channel 3 ($V(t_3) > 10$ mV), on towed array data collected on the RR and the 20-mm RF. In December 2005, ground-truth data were collected over three of the grids at the RR (Figure 3) and one grid at the 20-mm RF (Figure 4). A total of 458 ground-truth items were recovered, and are summarized in Table 1. The list contains 40 MEC with caliber greater than 20 mm, 77 projectiles (20-mm) and 20 emplaced 37-mm rounds. These rounds were emplaced by Sky Research personnel to test the detection and discrimination characteristics of the towed array.

This validation exercise was useful to this demonstration in several ways. First, it allowed testing the feasibility of the ground-truth collection methodology. Second, it provided valuable information on the number and distribution of MEC within the survey area. The highest concentration of anomalies and of MEC occurred around Grid K-13.

Counting the number of towed array anomalies with $V(t_3) > 10$ mV in each grid of the Rocket Range (Figure 3 and Table 2) reveals that Grids L-13 to 15, K-14 to 15, and I-12 to 13 have relatively high anomaly densities. As these are close to Grid K-13 where many MEC were found, demonstration efforts were focused in that area. The specific intent was to collect data on the eight grids outlined in red in Figure 3 and itemized in Table 2. On arriving at the site in early June 2006, it was discovered that Grid K-14 had already been cleared by the incumbent explosive ordnance disposal (EOD) contractor. Grid L-13 was therefore substituted for Grid K-14.

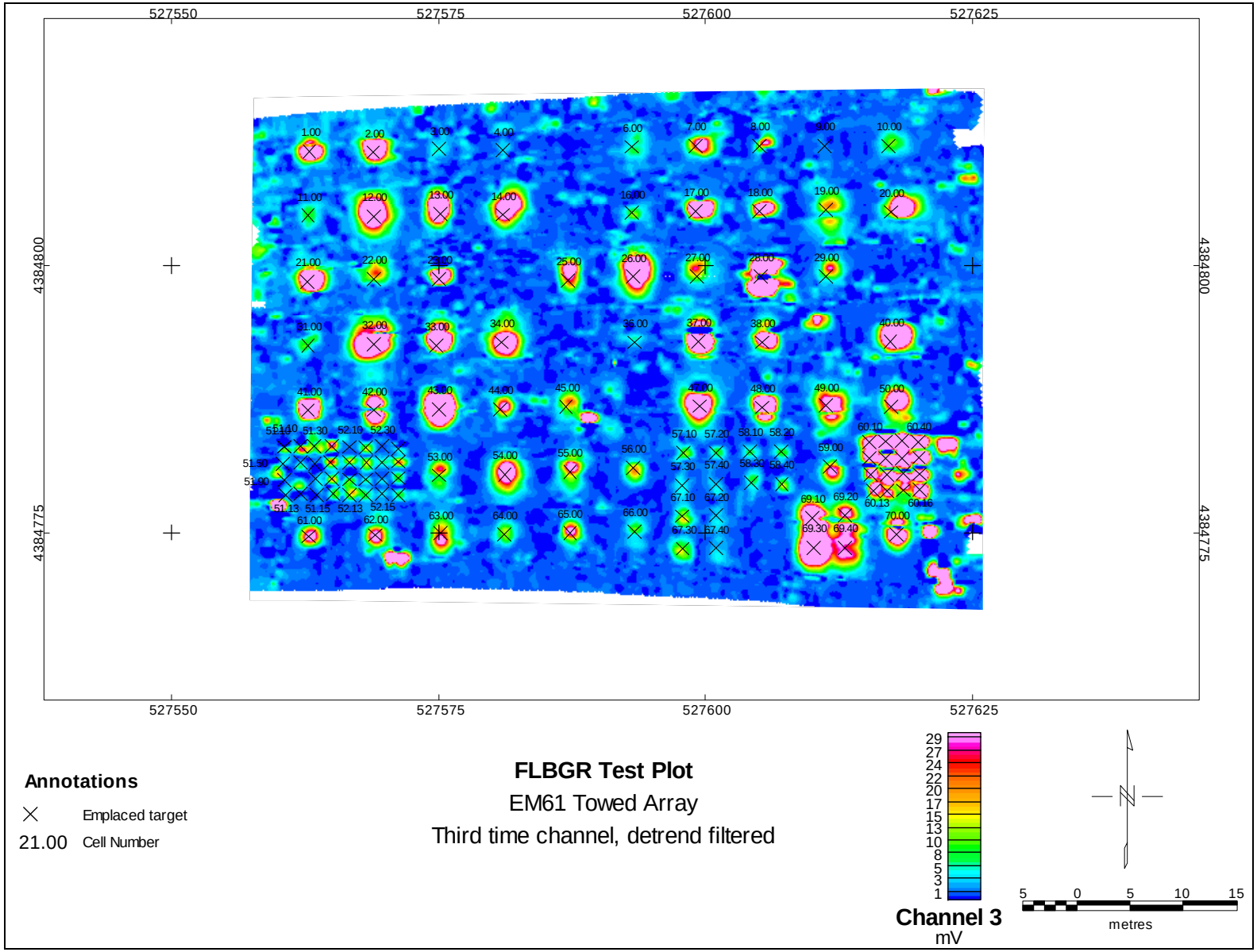


Figure 2. Map of time channel 3 of the EM-61 survey of the FLBGR test plot with emplaced items overlain.

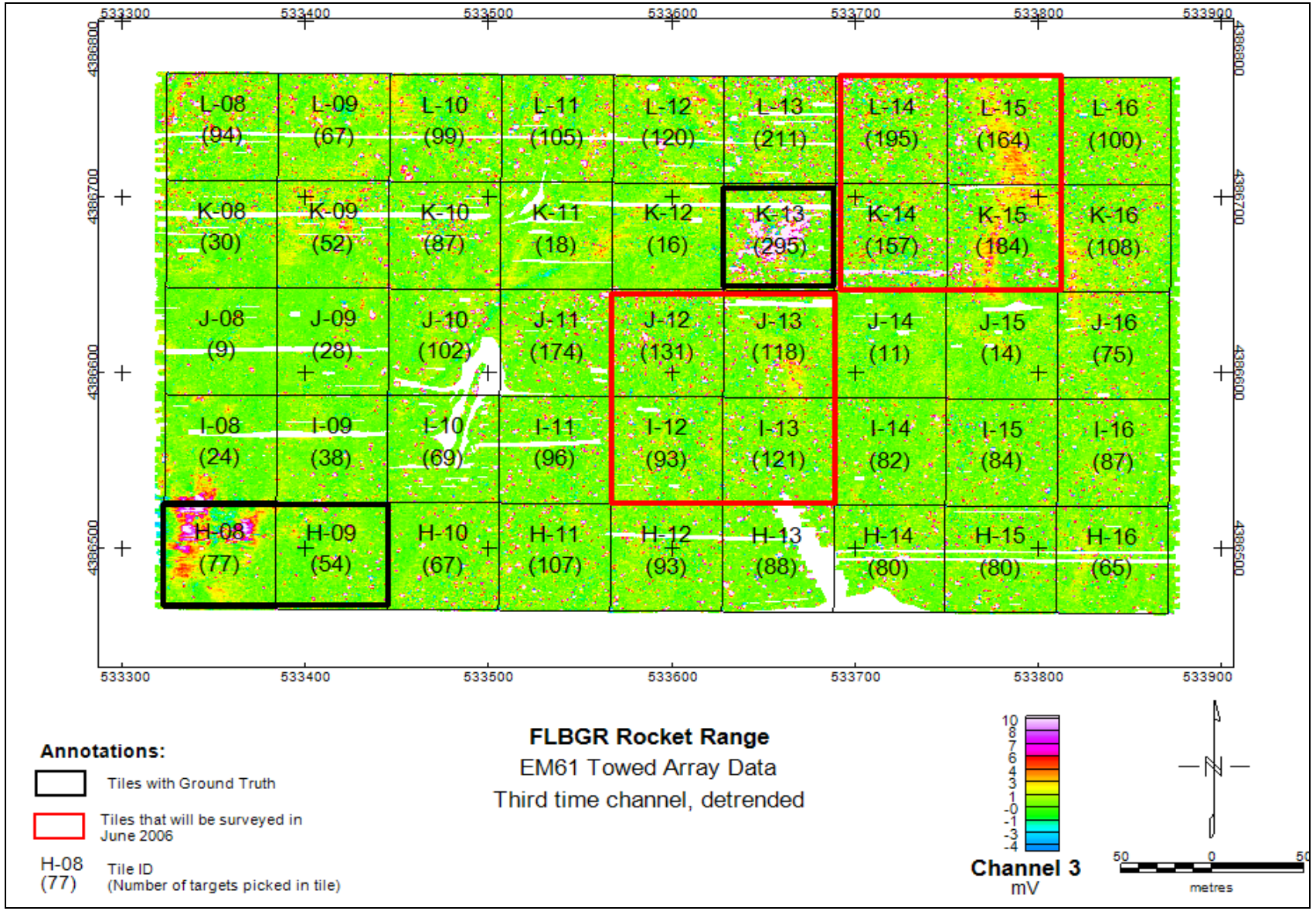


Figure 3. Map of Rocket Range with areas surveyed for this demonstration outlined in red.

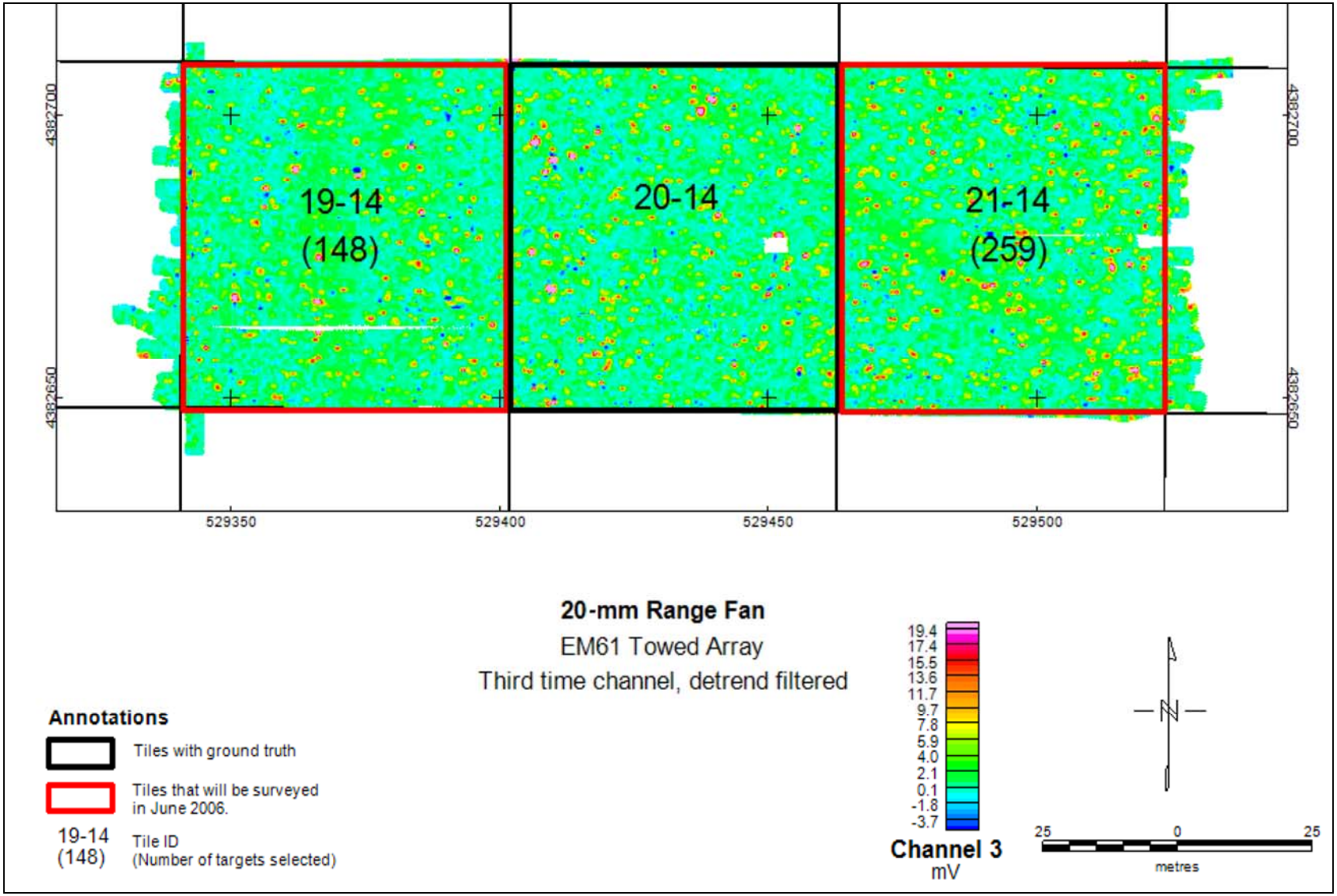


Figure 4. Map of the 20-mm Range Fan, with the two grids surveyed for this demonstration outlined in red.

Table 1. Summary of ground-truth items recovered during excavations at three Rocket Range and one 20-mm Range Fan grid in 2005.

| Anomaly | 20-14 | H-8 | H-9 | K-13 | Total |
|---|---|---|---|---|---|
| Bomb M50 Incendiary (4 lb) | | | 2 | | 2 |
| Bomb M-38 Practice (100 lb) | | | 1 | | 1 |
| Bomb MK-34 Practice | | | | 1 | 1 |
| Bomb MK-23 Practice (3 lb) | | | | 34 | 34 |
| Projectile 57-mm HEAT | | | 1 | 1 | 2 |
| Projectile 37-mm (emplaced) | 6 | | 7 | 7 | 20 |
| Projectile 20-mm | 25 | 6 | 14 | 32 | 77 |
| Shrapnel/fragmentation | | 7 | 16 | 83 | 106 |
| Small arms | 37 | 1 | | | 38 |
| Non-Military Scrap/Junk | 1 | 2 | 4 | 129 | 136 |
| Nothing Found | | 17 | 6 | 18 | 41 |
| Total | 69 | 33 | 51 | 305 | 458 |

Table 2. Number of anomalies selected with amplitudes above 10 mV in the third time channel of the Sky Research towed array EM-61 data.

| Grid | Number Targets | Comments |
|---|---|---|
| I-12 | 93 | Medium density |
| I-13 | 121 | Medium density |
| J-12 | 131 | Medium density |
| J-13 | 118 | Medium density |
| K-14 (not used) | 157 | High density |
| K-15 | 184 | High density and geology |
| L-13 (replaced K-14) | 211 | High density |
| L-14 | 195 | High density |
| L-15 | 164 | High density and geology |
| Total (RR) | 1,217 | Does not include K-14 |
| 19-14 | 148 | Medium density |
| 21-14 | 259 | High density |
| Total (20mmRF) | 407 | |
| Total (All) | 1,624 | Does not include K-14 |

Targets were selected using $V(t_3) > 10$ mV in each grid of the 20-mm Range Fan (Figure 4 and Table 2). This target selection reveals that grid 21-14 has a considerably higher concentration of anomalies than grid 19-14. Both of these grids were used for this demonstration.

## 2.3. Discrimination mode surveys conducted at FLBGR

Three different discrimination mode surveys were conducted on the eight RR grids and the two grids in the 20-mm RF:

1. Geonics EM-61 towed array with Leica RTS and Crossbow AHRS-400 IMU for position and orientation (September to October 2005);
2. Geonics EM-63 cart with Leica RTS and Crossbow AHRS-400 IMU for position and orientation (June to July 2006); and
3. Geometrics G823 cesium vapor, quad-sensor magnetometer array with Leica RTS and Crossbow AHRS-400 IMU for position and orientation (June 2006).

More details on these surveys can be found in the ESTCP-MM0504 demonstration report (Billings et al. 2007).

## 2.4. Cued-interrogation surveys conducted at FLBGR

Two different cued-interrogation surveys were conducted at FLBGR, including:

1. Geonics EM-63 cart with Leica RTS and Crossbow AHRS-400 IMU for position and orientation (July 2006). Data were collected over 28 anomalies in the Rocket Range and over 17 emplaced 37-mm projectiles on the 20-mm Range Fan.
2. GEM-3 template (June 2006) over 59 anomalies on the 20-mm Range Fan.

### 2.4.1. Cued interrogation with the EM-63

Cued-interrogation data were collected along parallel transects spaced 25 centimeters (cm) apart, with one line collected in an orthogonal direction over the estimated anomaly center. These lanes were pre-marked on a 2.5-meter (m) by 2.5-m tarpaulin (Figure 5) with data generally collected over a 3-m by 3-m square area centered on the estimated anomaly location. To maximize the signal-to-noise ratio (SNR) and to minimize high-frequency vibrations, the same EM-63 suspension cart and RTS/IMU combination that was used for the discrimination mode data collection was again employed.

Figure 5. Tarpaulin with marked lanes for cued interrogation (on right) and the EM-63 collecting calibration data while on two plastic sawhorses (on left).

Data collection was conducted in July 2007 over 17 emplaced 37-mm projectiles in the 20-mm RF and 28 unknown items in the RR (grids I12 and J13). These included five MK-23 practice bombs, seven 20-mm projectiles, and 16 other items such as shrapnel and junk (Table 3). Each day data were collected over approximately 15 items, which represents a relatively low rate of production. When the same system was deployed to Camp Sibert in May 2007 as part of the UXO Discrimination Study conducted under project ESTCP MM-0504, production rates of approximately 40 anomalies per day were found to be realistic.

### 2.4.2. Cued interrogation with the GEM-3

Measurements collected in 2005 with the Geophex GEM-3 with the 40-centimeter (cm) head demonstrated that the instrument had good performance against small objects. Therefore, the GEM-3 was used for cued interrogation of small objects such as 37-mm projectiles. After testing a number of data collection methods, a 1-m by 1-m template consisting of 49 measurement locations was selected. A schematic of the template is shown in Figure 6. Approximately five seconds of data were collected at each location on the template (Figure 7a). At the 50th survey location, a fiberglass jig, data were collected at a second elevation (3 cm higher) in the center of the template (Figure 7b).

Table 3: List of anomalies surveyed with the EM-63 in cued-interrogation mode. The item location is provided in UTM coordinates Zone 11, NAD-83, and the estimated depth (to the item center) is in centimeters.

| Label | Grid | Easting (m) | Northing (m) | Depth (cm) | Item |
|---|---|---|---|---|---|
| 1 | 19-14 | 529369.09 | 4382694.46 | 3 | Projectile 37-mm (emplaced) |
| 2 | 19-14 | 529389.05 | 4382691.54 | 0 | Projectile 37-mm (emplaced) |
| 3 | 19-14 | 529350.22 | 4382678.01 | 14 | Projectile 37-mm (emplaced) |
| 4 | 19-14 | 529395.65 | 4382672.99 | 9 | Projectile 37-mm (emplaced) |
| 5 | 19-14 | 529369.84 | 4382673.20 | 14 | Projectile 37-mm (emplaced) |
| 6 | 19-14 | 529361.18 | 4382666.23 | 15 | Projectile 37-mm (emplaced) |
| 7 | 19-14 | 529378.25 | 4382660.87 | 10 | Projectile 37-mm (emplaced) |
| 8 | 21-14 | 529488.50 | 4382705.55 | 19 | Projectile 37-mm (emplaced) |
| 9 | 21-14 | 529506.06 | 4382706.49 | 17 | Projectile 37-mm (emplaced) |
| 10 | 21-14 | 529475.81 | 4382691.12 | 18 | Projectile 37-mm (emplaced) |
| 11 | 21-14 | 529494.05 | 4382689.99 | 13 | Projectile 37-mm (emplaced) |
| 12 | 21-14 | 529480.90 | 4382668.43 | 18 | Projectile 37-mm (emplaced) |
| 13 | 21-14 | 529514.23 | 4382666.79 | 30 | Projectile 37-mm (emplaced) |
| 14 | 21-14 | 529487.05 | 4382656.85 | 25 | Projectile 37-mm (emplaced) |
| 15 | 21-14 | 529497.57 | 4382656.44 | 18 | Projectile 37-mm (emplaced) |
| 16 | 21-14 | 529524.30 | 4382661.33 | 23 | Projectile 37-mm (emplaced) |
| 17 | 21-14 | 529525.22 | 4382703.12 | 23 | Projectile 37-mm (emplaced) |
| 18 | I12 | 533576.93 | 4386574.53 | 10 | Shrapnel |
| 19 | I12 | 533579.07 | 4386554.31 | 10 | Shrapnel |
| 20 | I12 | 533577.00 | 4386571.47 | 0 | Bomb MK-23 Practice (3 lb) |
| 21 | I12 | 533597.86 | 4386582.61 | 12 | Projectile 20-mm |
| 22 | I12 | 533566.68 | 4386525.43 | 0 | Junk |
| 23 | I12 | 533600.05 | 4386559.50 | 0 | Shrapnel |
| 24 | I12 | 533608.24 | 4386552.70 | 0 | Projectile 20-mm |
| 25 | I12 | 533566.42 | 4386553.64 | 15 | Shrapnel |
| 26 | I12 | 533627.49 | 4386535.27 | 8 | Bomb MK-23 Practice (3 lb) |
| 27 | I12 | 533606.54 | 4386571.75 | 0 | Small arms |
| 28 | I12 | 533605.83 | 4386540.50 | 25 | Projectile 20-mm |
| 29 | I12 | 533610.57 | 4386531.94 | 8 | Bomb MK-23 Practice (3 lb) |
| 30 | I12 | 533615.04 | 4386554.33 | 6 | Shrapnel |
| 31 | I12 | 533601.96 | 4386560.75 | 12 | Projectile 20-mm |
| 32 | I12 | 533582.72 | 4386556.53 | 25 | Shrapnel |
| 33 | I12 | 533597.67 | 4386581.98 | 2 | Projectile 20-mm |
| 34 | I12 | 533590.42 | 4386543.12 | 6 | Projectile 20-mm |
| 35 | I12 | 533591.01 | 4386576.12 | 7 | Projectile 20-mm |
| 36 | I12 | 533578.66 | 4386538.47 | 3 | Shrapnel |
| 37 | J13 | 533653.19 | 4386602.85 | 0 | Shrapnel |
| 38 | J13 | 533627.36 | 4386624.33 | 0 | Bomb MK-23 Practice (3 lb) |
| 39 | J13 | 533651.64 | 4386594.47 | 12 | Shrapnel |
| 40 | J13 | 533634.71 | 4386646.60 | 10 | Shrapnel |
| 41 | J13 | 533653.66 | 4386593.11 | 8 | Shrapnel |
| 42 | J13 | 533682.78 | 4386596.36 | 2.54 | Shrapnel |
| 43 | J13 | 533656.02 | 4386596.76 | 0 | Bomb MK-23 Practice (3 lb) |
| 44 | J13 | 533665.42 | 4386644.43 | 6 | Junk |
| 45 | J13 | 533651.51 | 4386597.98 | 5 | Shrapnel |

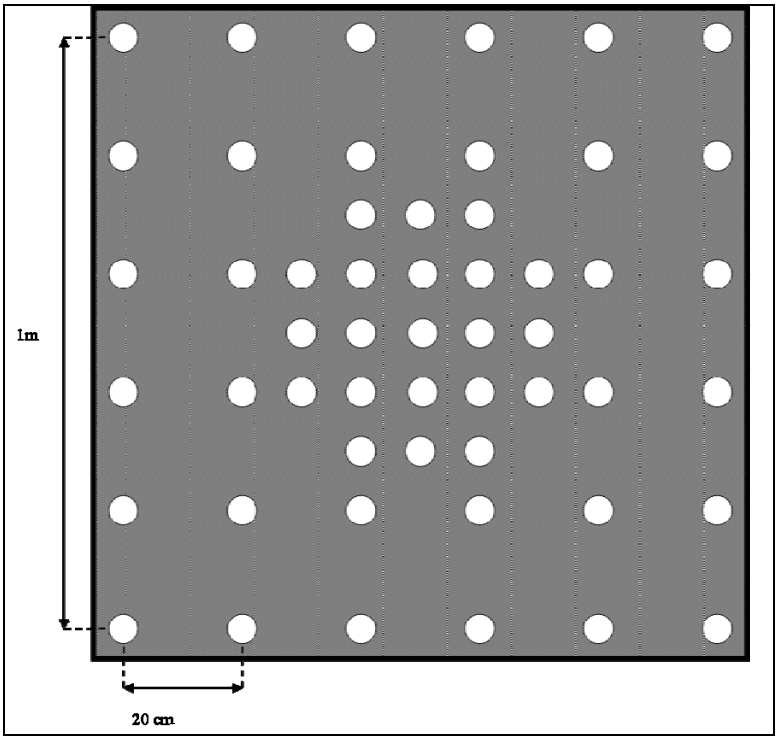


Figure 6. Schematic of the template used for GEM surveying. The 36 holes in the main grid are separated by 20 cm. The center of the template contains 17 extra holes to increase the density to 10 cm directly over the target. The four corners of the template were not surveyed. This resulted in 49 survey locations.

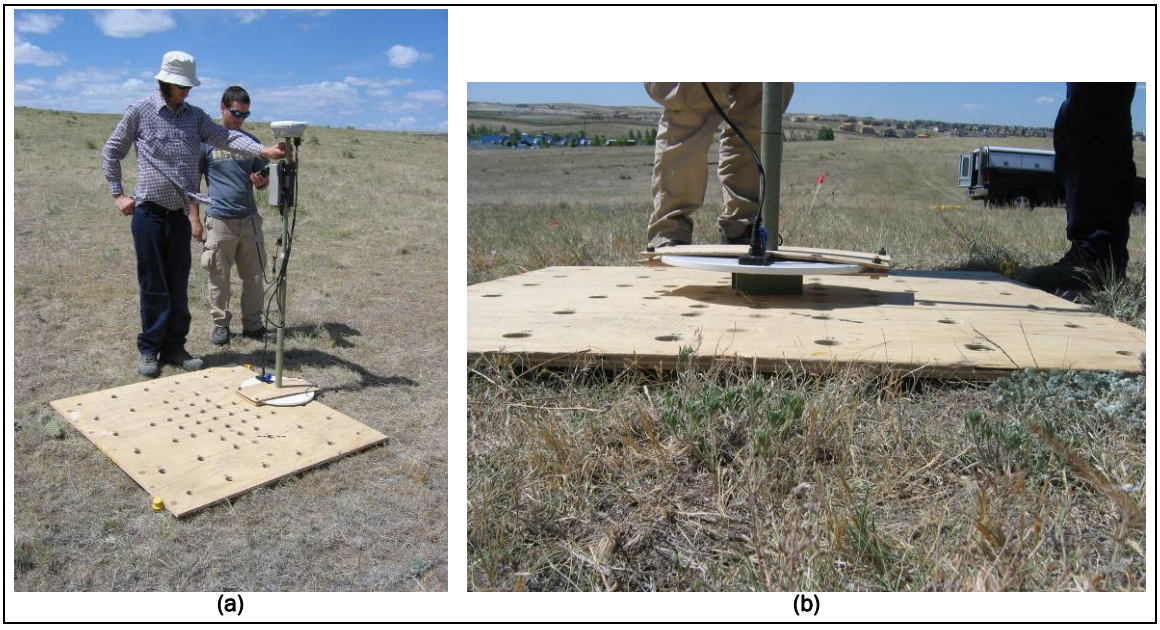

(a) (b)

Figure 7. GEM-3 collecting cued-interrogation data at the 20-mm Range Fan. Photo on right is a fiberglass jig that is used to collect data at a second elevation (3 cm above template) at the center of the template.

The GEM-3 data were collected in May 2006 over 41 anomalies in grid 19-14 and 18 anomalies in grid 21-14, both of which are in the 20-mm RF. The anomalies comprised 15 small arms, 23 projectiles (20-mm), 19 emplaced 37-mm projectiles, and one 37-mm HE projectile (Table 4).

Table 4. Anomalies surveyed with the GEM-3 in a cued-interrogation mode.

| Label | Grid | Easting (m) | Northing (m) | Depth (cm) | Item |
|---|---|---|---|---|---|
| 1 | 19-14 | 529385.06 | 4382682.75 | 5 | Projectile 20-mm |
| 2 | 19-14 | 529373.70 | 4382689.50 | 2 | Projectile 20-mm (multiple) |
| 3 | 19-14 | 529383.27 | 4382694.36 | 2 | Projectile 20-mm |
| 4 | 19-14 | 529366.08 | 4382667.34 | 18 | Projectile 37-mm (emplaced) |
| 5 | 19-14 | 529388.07 | 4382662.40 | 10 | Projectile 20-mm |
| 6 | 19-14 | 529386.46 | 4382677.36 | 11 | Projectile 20-mm |
| 7 | 19-14 | 529356.37 | 4382686.81 | 28 | Projectile 37-mm (emplaced) |
| 8 | 19-14 | 529351.14 | 4382707.20 | 30 | Projectile 20-mm |
| 9 | 19-14 | 529362.90 | 4382698.33 | 3 | Projectile 20-mm |
| 10 | 19-14 | 529361.86 | 4382690.13 | 7 | Projectile 20-mm |
| 11 | 19-14 | 529389.85 | 4382659.46 | 10 | Projectile 20-mm |
| 12 | 19-14 | 529376.43 | 4382676.11 | 2 | Projectile 20-mm |
| 13 | 19-14 | 529378.50 | 4382671.26 | 5 | 50 cal |
| 14 | 19-14 | 529393.24 | 4382654.78 | 10 | 50 cal (multiple) |
| 15 | 19-14 | 529396.09 | 4382678.84 | 12 | Projectile 20-mm |
| 16 | 19-14 | 529356.21 | 4382683.33 | 6 | 50 cal |
| 17 | 19-14 | 529366.17 | 4382674.66 | 34 | Projectile 37-mm HE |
| 18 | 19-14 | 529345.14 | 4382701.16 | 4 | 50 cal (60cm from flag) |
| 19 | 19-14 | 529399.82 | 4382656.05 | 2 | 50 cal |
| 20 | 19-14 | 529398.43 | 4382662.94 | 4 | 50 cal |
| 21 | 19-14 | 529344.97 | 4382659.24 | 10 | Projectile 20-mm |
| 22 | 19-14 | 529394.44 | 4382682.93 | 5 | Projectile 20-mm |
| 23 | 19-14 | 529377.73 | 4382685.27 | 8 | 50 cal |
| 24 | 19-14 | 529401.38 | 4382687.50 | 5 | 50 cal |
| 25 | 19-14 | 529381.37 | 4382677.32 | 3 | 50 cal |
| 26 | 19-14 | 529391.60 | 4382675.78 | 4 | 50 cal |
| 27 | 19-14 | 529341.07 | 4382705.64 | 2 | 50 cal |
| 28 | 19-14 | 529401.50 | 4382681.13 | 5 | 50 cal |
| 29 | 19-14 | 529365.65 | 4382660.33 | 5 | 50 cal |
| 30 | 19-14 | 529365.66 | 4382657.03 | 5 | Projectile 20-mm |
| 31 | 19-14 | 529338.35 | 4382705.38 | 7 | Projectile 20-mm |
| 32 | 19-14 | 529352.88 | 4382702.88 | 10 | Projectile 37-mm (emplaced) |
| 33 | 19-14 | 529367.27 | 4382703.34 | 11 | Projectile 37-mm (emplaced) |
| 34 | 19-14 | 529391.03 | 4382706.44 | 13 | Projectile 37-mm (emplaced) |

| Label | Grid | Easting (m) | Northing (m) | Depth (cm) | Item |
|---|---|---|---|---|---|
| 35 | 19-14 | 529369.10 | 4382694.47 | 10 | Projectile 37-mm (emplaced) |
| 36 | 19-14 | 529389.19 | 4382691.65 | 8 | Projectile 37-mm (emplaced) |
| 37 | 19-14 | 529350.23 | 4382678.03 | 16 | Projectile 37-mm (emplaced) |
| 38 | 19-14 | 529395.66 | 4382673.02 | 16 | Projectile 37-mm (emplaced) |
| 39 | 19-14 | 529369.82 | 4382673.13 | 18 | Projectile 37-mm (emplaced) |
| 40 | 19-14 | 529361.04 | 4382666.31 | 16 | Projectile 37-mm (emplaced) |
| 41 | 19-14 | 529378.17 | 4382660.81 | 16 | Projectile 37-mm (emplaced) |
| 42 | 21-14 | 529468.41 | 4382655.12 | 15 | Projectile 37-mm (emplaced) |
| 43 | 21-14 | 529482.17 | 4382671.11 | 10 | Projectile 20-mm |
| 44 | 21-14 | 529491.51 | 4382670.14 | 7 | Projectile 20-mm |
| 45 | 21-14 | 529468.61 | 4382658.65 | 8 | Projectile 20-mm |
| 46 | 21-14 | 529505.90 | 4382675.76 | 7 | Projectile 20-mm |
| 47 | 21-14 | 529477.59 | 4382648.07 | 5 | Projectile 20-mm |
| 48 | 21-14 | 529503.63 | 4382698.14 | 5 | Projectile 20-mm |
| 49 | 21-14 | 529465.93 | 4382696.61 | 15 | Projectile 20-mm |
| 50 | 21-14 | 529496.67 | 4382673.75 | 26 | Projectile 37-mm (emplaced) |
| 51 | 21-14 | 529480.36 | 4382693.47 | 7 | Projectile 20-mm |
| 52 | 21-14 | 529523.31 | 4382681.94 | 10 | Projectile 20-mm |
| 53 | 21-14 | 529510.59 | 4382697.88 | 2 | 50 cal |
| 54 | 21-14 | 529471.56 | 4382672.89 | 7 | 50 cal |
| 55 | 21-14 | 529467.44 | 4382673.48 | 22 | Projectile 37-mm (emplaced) |
| 56 | 21-14 | 529488.51 | 4382705.54 | 24 | Projectile 37-mm (emplaced) |
| 57 | 21-14 | 529505.98 | 4382706.39 | 24 | Projectile 37-mm (emplaced) |
| 58 | 21-14 | 529494.02 | 4382689.96 | 23 | Projectile 37-mm (emplaced) |
| 59 | 21-14 | 529480.89 | 4382668.50 | 24 | Projectile 37-mm (emplaced) |

# 3 Comparison of EM-63 Cued and Discrimination Mode Surveys

## 3.1. Comparison of data

Discrimination mode data were collected along parallel transects nominally spaced 0.5 m apart, with measurements spaced 0.1 to 0.2 m apart along each transect. The operator attempted to maintain a straight path between the start and end of the grid using visual markers, but there were considerable variations in the actual transect separation (Figures 8a and 9a). This meant that there were often significant variations in the measurement density and the amount of data available to constrain the dipole inversion. The cued-interrogation data had the advantage of higher and more consistent data density (Figures 8b and 9b) with the data collected by pushing the cart slowly along lines nominally spaced 0.25 m apart. In addition, an extra line of data was collected in a perpendicular direction over the anomaly center (Figure 8b). The short length of the cued-interrogation surveys meant that across-line sample spacing was very consistent, and the slow speed of survey resulted in measurement spacing between 0.05 and 0.1 m apart. The slow speed of forward traverse also resulted in less vibration, pitch, and roll in the cued-interrogation data, which would improve the ability of the data to constrain the parameters of the buried object.

## 3.2. Comparison of inversion results

Three-dipole Pasion-Oldenburg models (Pasion and Oldenburg 2001)

$$L_i(t) = k_i \left(t + \alpha_i\right)^{-\beta_i} \exp\left(-t / \gamma_i\right) \quad (1)$$

(with $\alpha_i = 0$ and $i = [1, 2, 3]$) were fit to both the discrimination and cued-interrogation mode datasets using the methods described in Report 6. The resulting fits were visually reviewed to determine if the model adequately represented the data. On the 20-mm RF, 16 of 17 of the cued-interrogation fits were deemed acceptable, compared to 15 of 15 for the discrimination

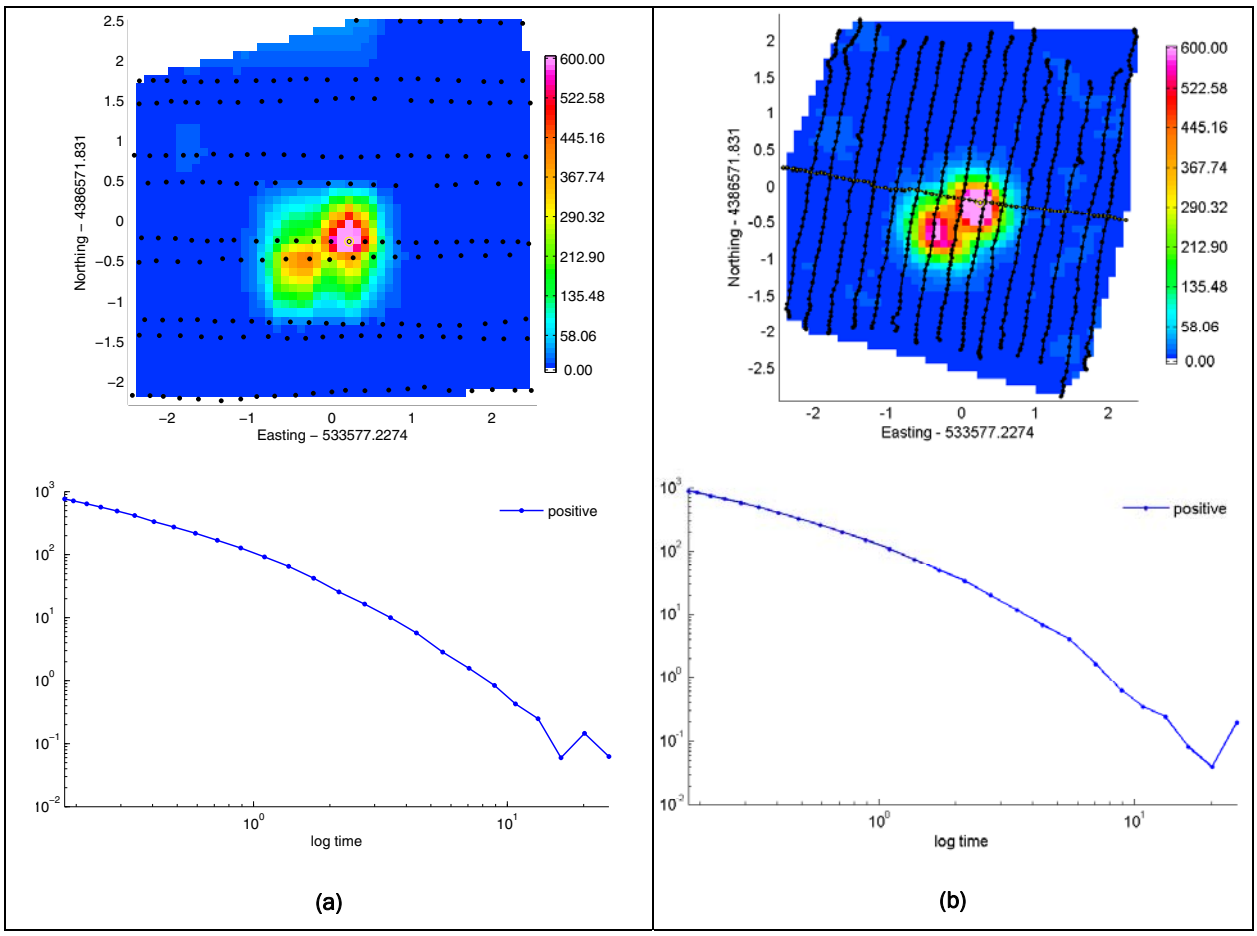


Figure 8: Comparison of time channel 1 from discrimination (a) and cued-interrogation (b) mode surveys of anomaly I12-1, an MK-23 practice bomb. The sounding at anomaly maximum is also shown.

mode data. At the RR, 27 of 28 cued-interrogation fits were accepted compared to 23 of 28 for the discrimination mode data. The lower acceptance rate at the RR for the discrimination mode data was due to the variable data coverage on that site.

Appendix A compares the inversion fits of the cued and discrimination mode data over two anomalies. The first is on anomaly I12-1 (an MK23 practice bomb) and the second over anomaly 2114-34 (a 37-mm projectile). Each inversion summary includes plan views of the data, model and residuals in time channels 1, 7, 14, and 21, along with a profile of each of those channels. Also included are the data and model sounding over the anomaly maximum, a plot of the polarization tensors, a table of polarization tensors, a summary of the fit parameters and a summary of the termination status from the optimization. The green polygon on the plan views represents the masks used to select the data submitted to the

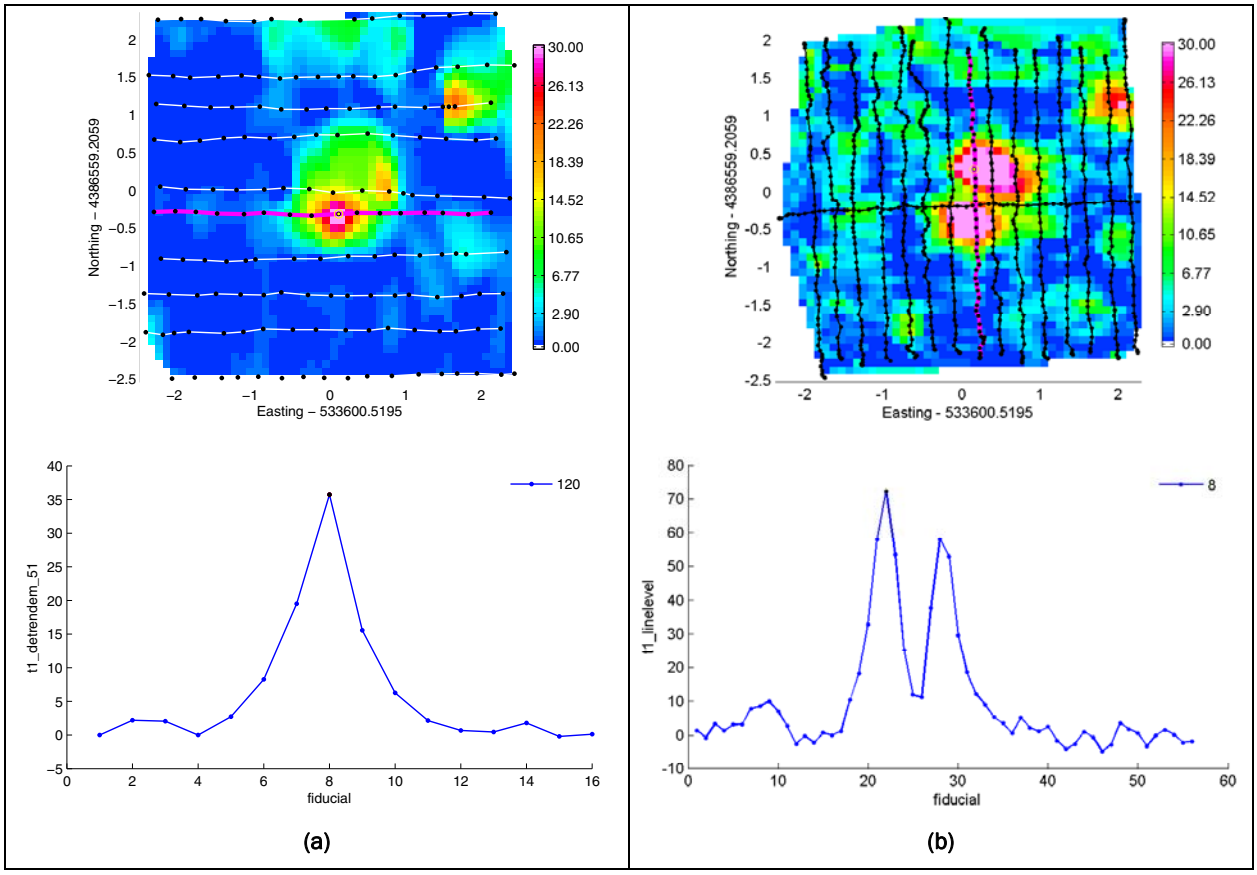


Figure 9: Comparison of time channel 1 from discrimination (left) and cued-interrogation mode surveys of anomaly I12-34, a large piece of ordnance debris. A profile along the target is also shown and emphasizes the much higher along-line sample rate of the cued-interrogation survey.

inversion, with the green stars on the profiles showing the intersection point of the mask on each transect. The red "Std Est" curve on the sounding plot shows the estimated noise level in each channel.

Considering the MK-23 practice bomb first, the much higher data density in the cued-interrogation data provides more stringent constraints on the spatial characteristics of the model. At early times, the transverse polarizations are predicted to be almost identical as one would expect from an axially symmetric object such as the MK-23. In contrast, the data density and quality in the discrimination mode data are not able to constrain the transverse polarizations and the object is predicted to be asymmetric.

For the 37-mm projectile, both survey types are able to constrain the model to be axially symmetric at early times. The main difference is that the cued-interrogation survey is better able to resolve the horizontal dipole than the discrimination mode survey, which has a large line-spacing near the anomaly center.

## 3.3. Analysis of feature vectors

The feature vectors recovered over both sets of data are compared in Figures 10 to 16. In terms of recovered positions, the discrimination mode data appear to be slightly more accurate, although the difference between the two methods is very small (Figure 10). There are a number of anomalies, with predicted locations more than 40 cm from the ground-truth location. For several of these locations, there are a number of nearby anomalies, and it is likely that the ground truth refers to one of those anomalies instead.

The predicted depths from the cued-interrogation data are in closer agreement with the ground-truth depths than is the case for the discrimination mode data (Figure 11). All cued-interrogation fits over MK-23 and 37-mm projectiles are within 7 cm of the true location, except one 37-mm projectile at 30 cm, which was predicted to be at 40.6 cm (Figure 11c).

Using the recovered Pasion-Oldenburg parameters, the polarization is calculated at the first time channel using Equation 1 and the results are plotted in Figure 12. The vertical axis in the (a) and (b) plots comprises the average of the secondary and tertiary parameters, with a vertical line joining the two values. An axially symmetric object would have $L_2(t_1) = L_3(t_1)$ and the line would collapse to a point, whereas asymmetric scrap may have significantly different values. The $L_1(t_1)$ and $L_2(t_1)$ values estimated from the 20- and 37-mm projectiles and the Mk-23 practice bombs are more tightly clustered for the cued-interrogation data. The predicted values for the 37-mm projectiles agree very well with values previously obtained from the ERDC test stand. In addition, the secondary and tertiary polarizations are very close together for the 37-mm projectiles and the MK-23 bombs, as expected for these radially symmetric objects (Figures 12c and 12d). In contrast, many of the fits to the same items using the discrimination mode data have significantly different secondary and tertiary polarizations. Thus, the spread feature vector appears to have good discrimination potential for the cued-interrogation data but not for the discrimination mode data. Notice also that the ratio of secondary to primary polarizations is more consistent for the cued-interrogation data.

Turning now to the Pasion-Oldenburg β and γ parameters (which are indicative of decay rate), Figure 13 compares the recovered values for the discrimination and cued-interrogation mode datasets. The primary β and γ parameters of the 37-mm projectiles are tightly clustered for both the

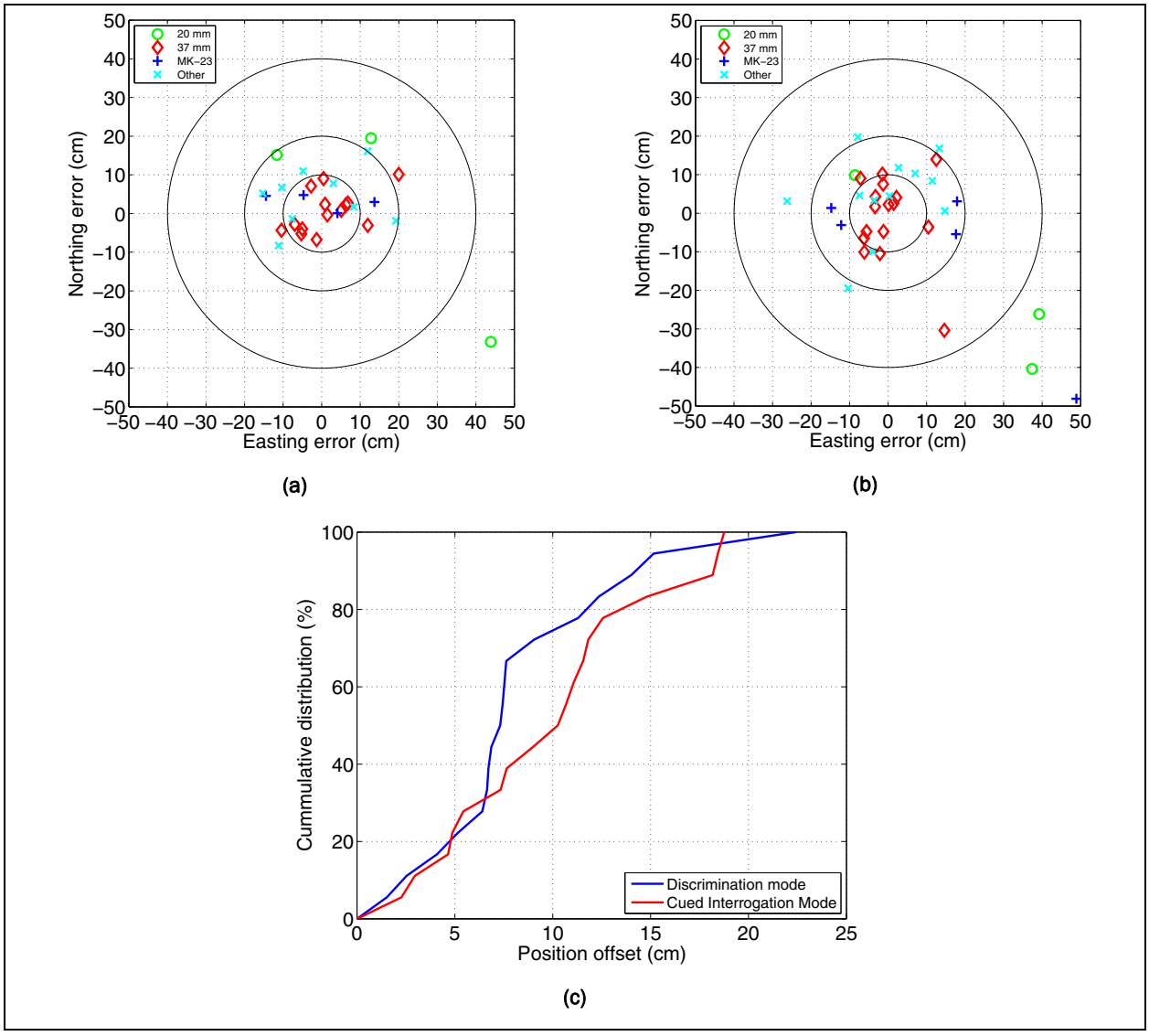


Figure 10. Comparison of predicted and ground-truth locations for the discrimination (a) and cued-interrogation mode (b) models. Also shown is a cumulative distribution function (c) of the position error for both survey types on the 37-mm and MK-23 projectiles. Surprisingly the discrimination mode models appear to be slightly better positioned, although the difference may not be significant.

discrimination and cued-interrogation datasets and agree well with previously obtained test-stand values. For the MK-23 practice bombs, the primary β and γ parameters are more tightly clustered for the cued-interrogation data. Parameter values recovered over the 20-mm projectiles and other items are widely dispersed, indicating that neither method is capable of accurately recovering the decay rate of the small 20-mm projectiles. For the secondary β and γ parameters, both methods exhibit much larger scatter. The values for the MK-23 practice bombs are similar to the cued-interrogation data, and a number of the 37-mm projectiles cluster around the value recovered from the test-stand data.

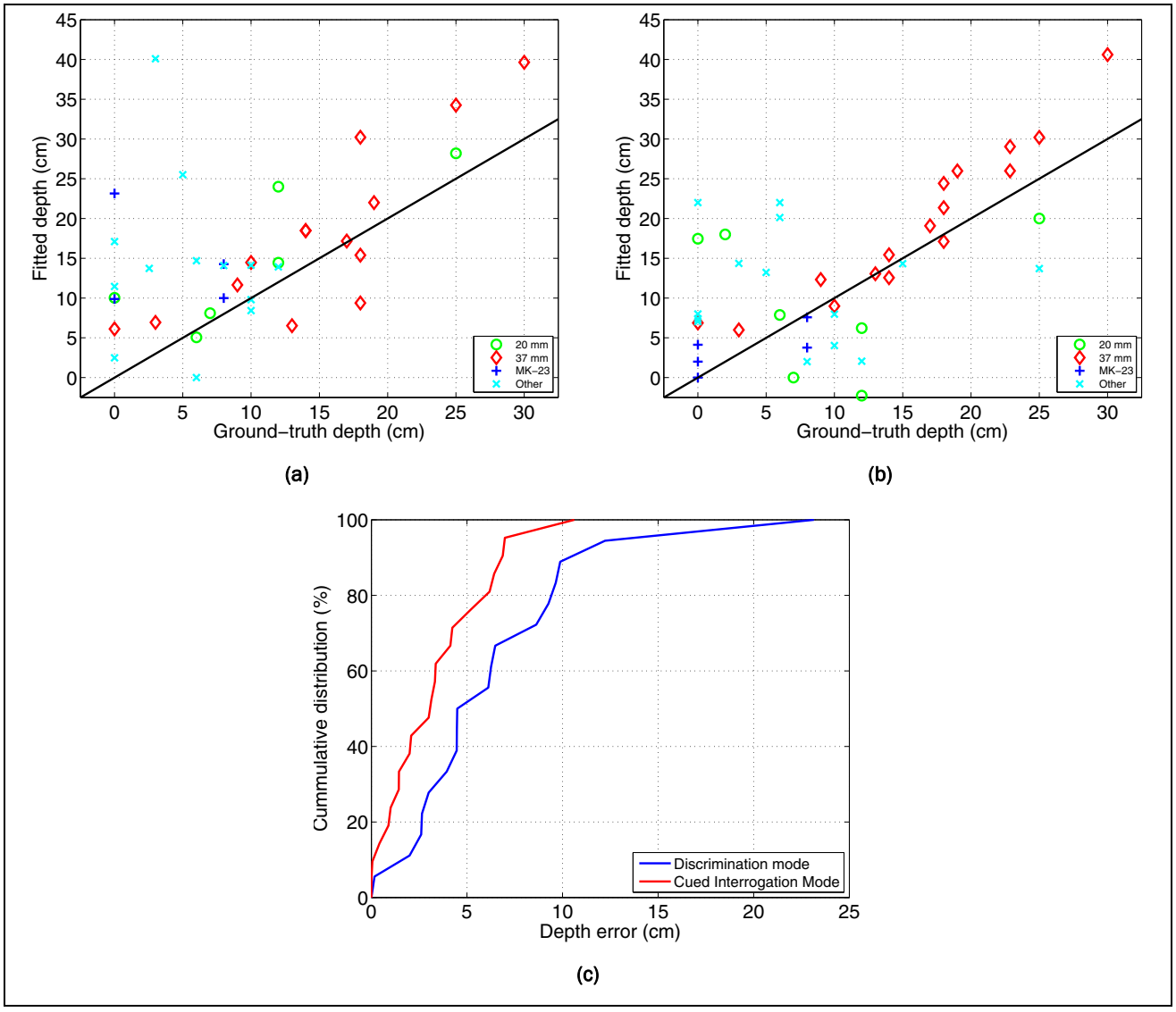


Figure 11. Comparison of predicted and ground-truth depths for the discrimination (a) and cued-interrogation mode (b) models. Also shown is a cumulative distribution function (c) of the depth error on the 37-mm and MK-23 projectiles.

The *relative decay rate at time channel n* is defined as the ratio of the polarization at time channel *n* to the polarization at time channel 1. This is often found to be a more useful discrimination diagnostic (Figure 14) of the decay behavior than the β and γ parameters. The relative decay rates at time channels 10 (0.72 ms) and 19 (5.6 ms) can be used to clearly distinguish all 37-mm projectiles from all the other items measured. The MK-23 practice bombs have a very rapid decay and cannot easily be separated from the other items using time-decay information. The parameter clustering for both UXOs is tighter for the cued-interrogation data.

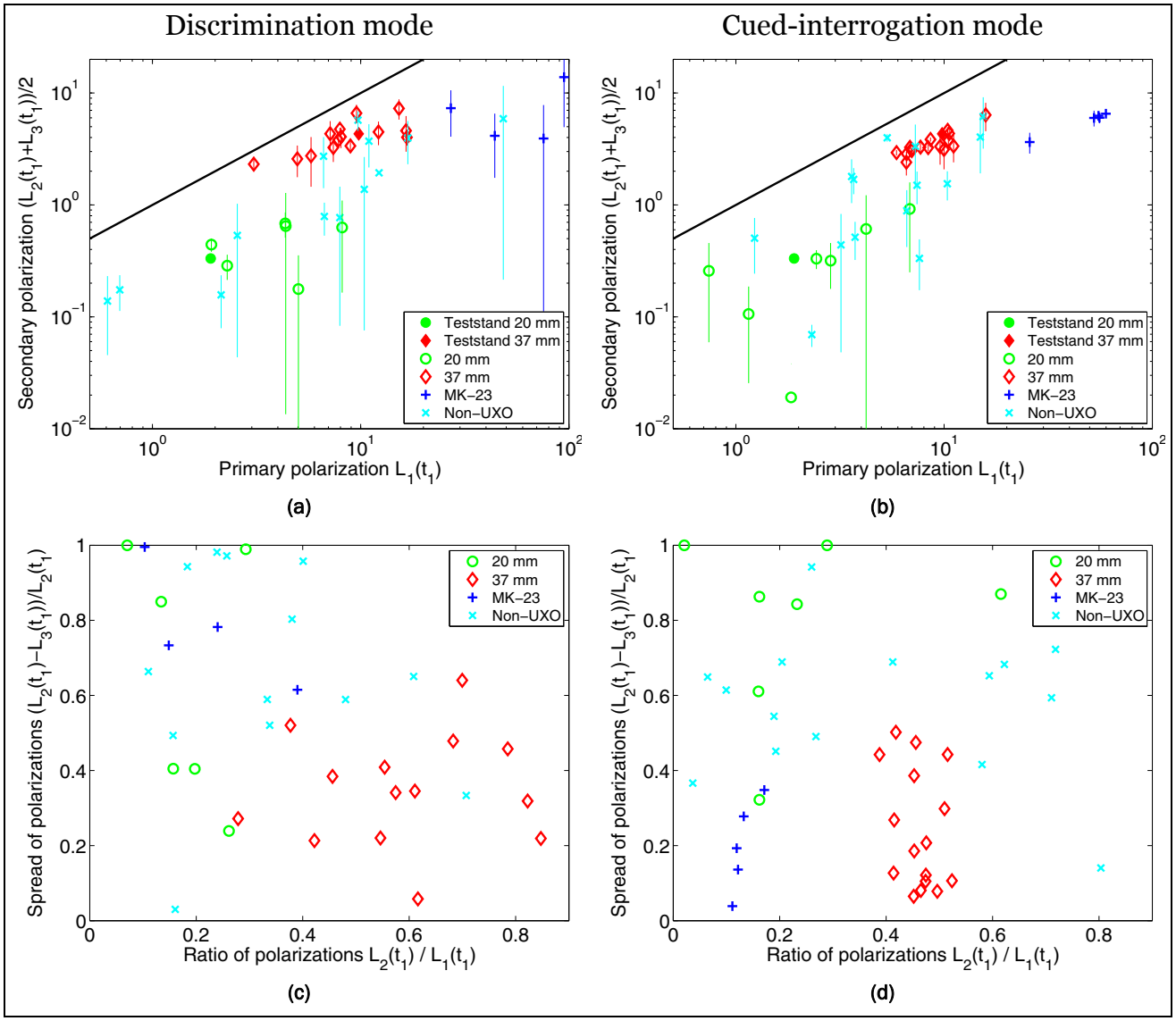


Figure 12. Predicted primary, secondary, and tertiary polarizations of Pasion-Oldenburg models fit to the discrimination [(a) and (c)] and cued-interrogation mode [(b) and (d)] data. For the secondary polarizations in (a) and (b), the averages of the two smaller polarizations were plotted, with a vertical line drawn between the two polarizations. Also shown are the predicted values for the 20- and 37-mm projectiles obtained by inverting test-stand data. In (c) and (d), the ratios of secondary to primary polarizations were compared against the spread in the secondary and tertiary polarizations.

Figures 15 and 16 compare the primary and secondary polarizations of the 20-mm, 37-mm, and MK-23 items recovered using discrimination and cued-interrogation data. These plots offer an alternative visualization of the information that was summarized in Figures 12 to 14. The wide scatter of the recovered polarizations over the 20-mm projectiles emphasizes the difficulty in resolving such small objects. For the 37-mm projectiles, it is evident that the primary polarizations are relatively well constrained by the cued-interrogation data and less so for the discrimination mode data.

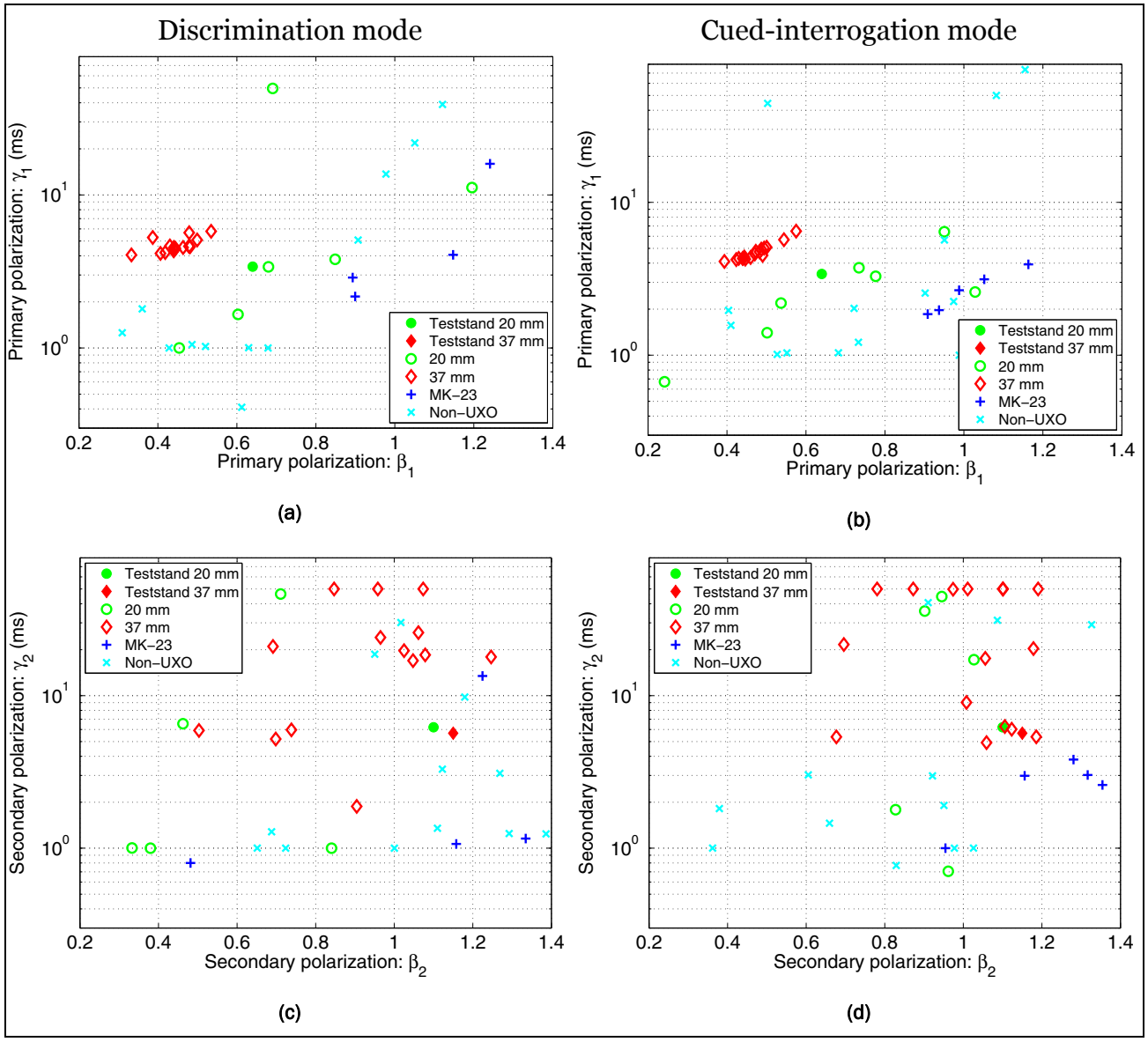


Figure 13: Predicted β and γ parameters for primary and secondary polarizations of Pasion-Oldenburg models fit to the discrimination [(a) and (c)] and cued-interrogation mode [(b) and (d)] data.

For the cued-interrogation data, the secondary polarizations of many of the 37-mm items are also fairly well constrained. There is a larger variation on the MK-23 practice bombs for both methods, although four of the five cued-interrogation anomalies have similar characteristics.

The relative decay curves (obtained by normalizing the polarizations by the value at the first time channel) indicate that there is very close agreement between all primary polarizations over all time channels for the 37-mm projectiles, particularly those obtained from the cued-interrogation data. The secondary polarizations are in good agreement

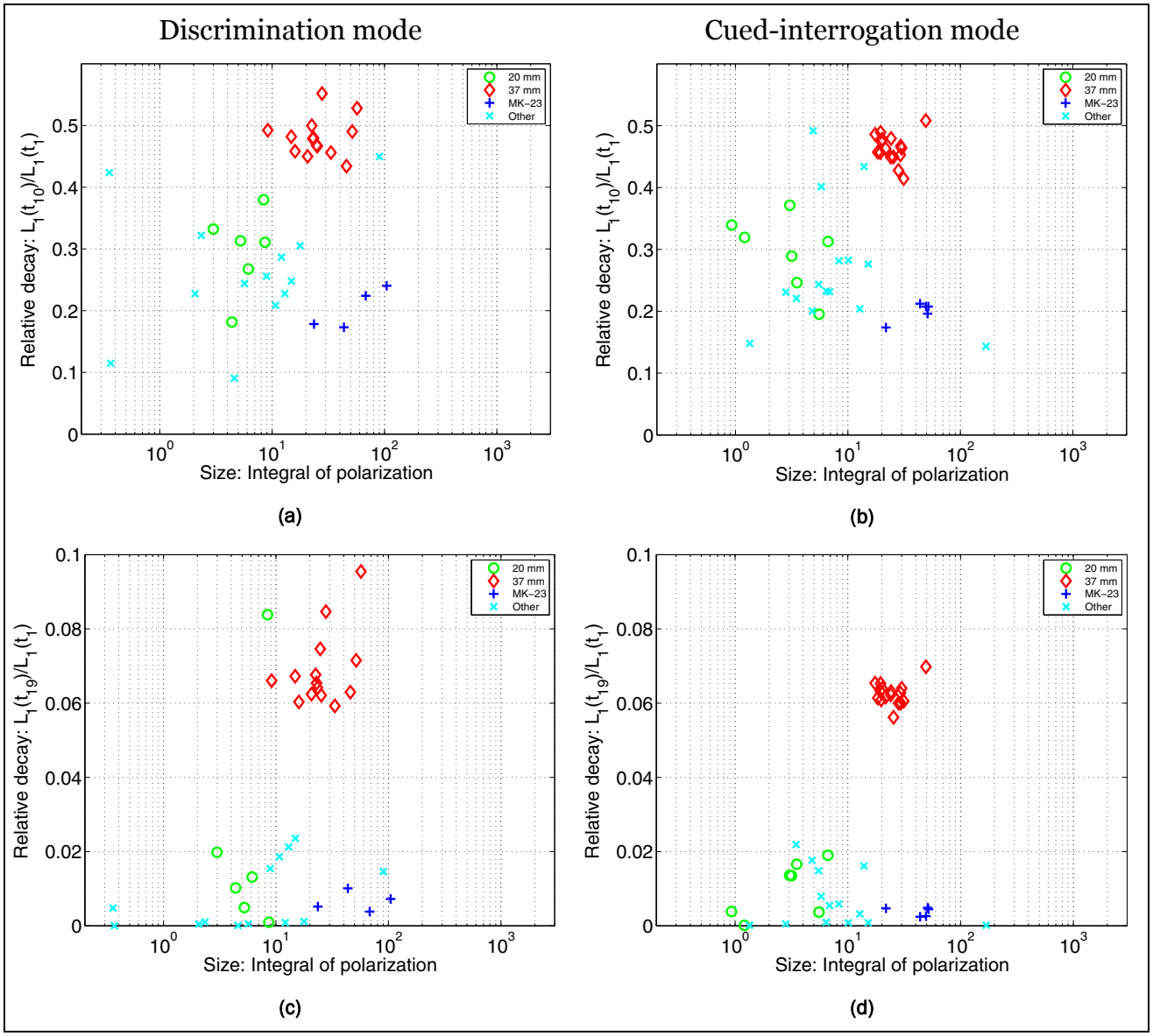


Figure 14. Predicted decay rates and size for the primary polarization of Pasion-Oldenburg models fit to the discrimination [(a) and (c)] and cued-interrogation mode [(b) and (d)] data. The size estimate is obtained by integrating the area under the polarization tensor curve, while the decay rates are calculated as the ratio of the response at channels 10 to 1 for (a) and (b) and channels 19 to 1 for (c) and (d).

out to about 2 ms, where they diverge significantly. The primary polarizations are in good agreement out to about 1 ms for the 20-mm projectiles and 2-3 ms for the MK-23 practice bombs. There is very poor agreement between secondary polarizations for the 20-mm projectiles on both datasets and the MK-23 practice bombs on the discrimination mode data. For the cued-interrogation mode data, the secondary polarizations of the MK-23 are in relatively close agreement.

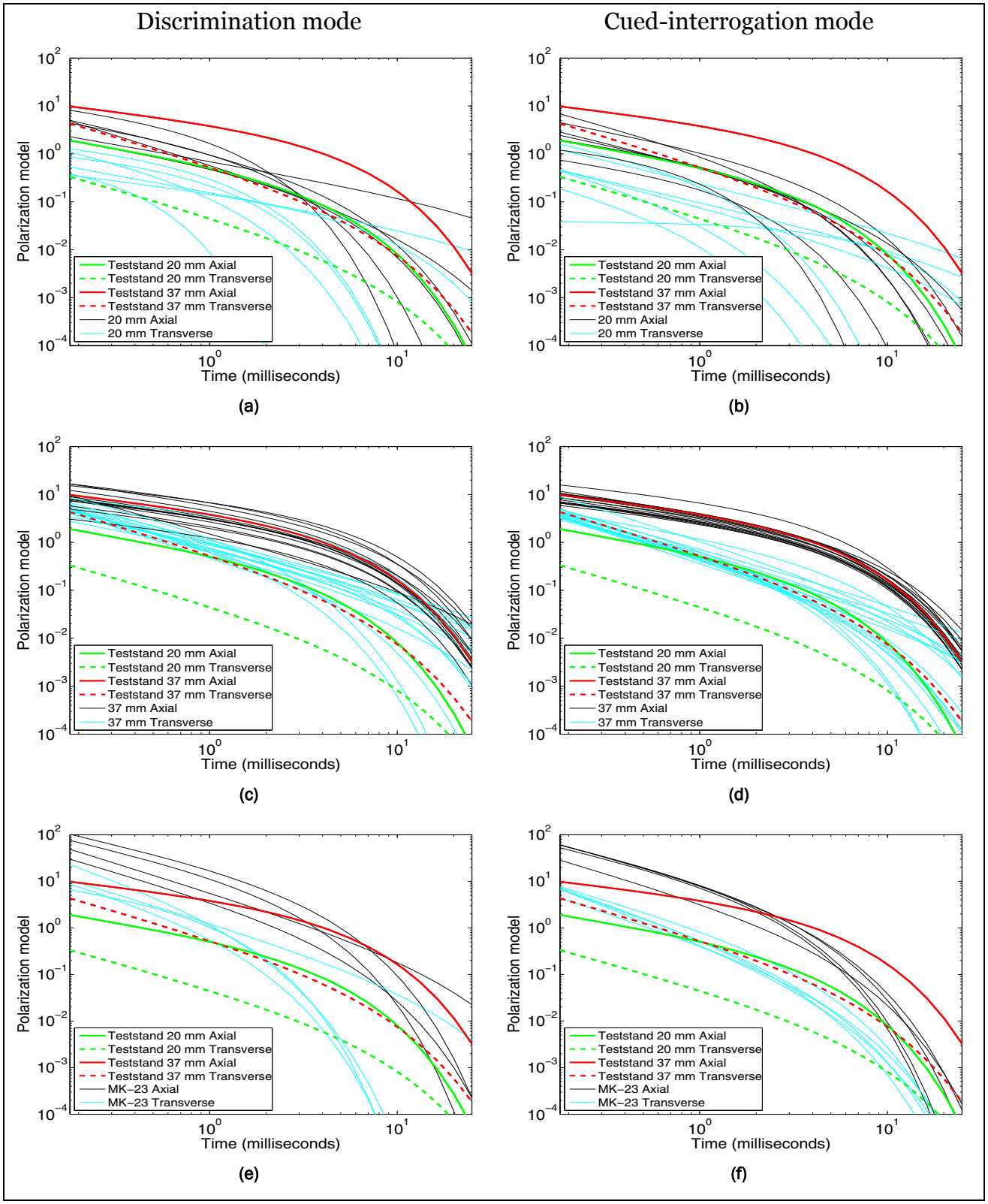


Figure 15. Primary (axial) and secondary (transverse) polarization tensor models recovered over 20- and 37-mm projectiles and MK-23 practice bombs. Results on the left are for discrimination mode data [(a), (c), and (e)], while results on the right are for cued-interrogation mode data [(b), (d), and (f)].

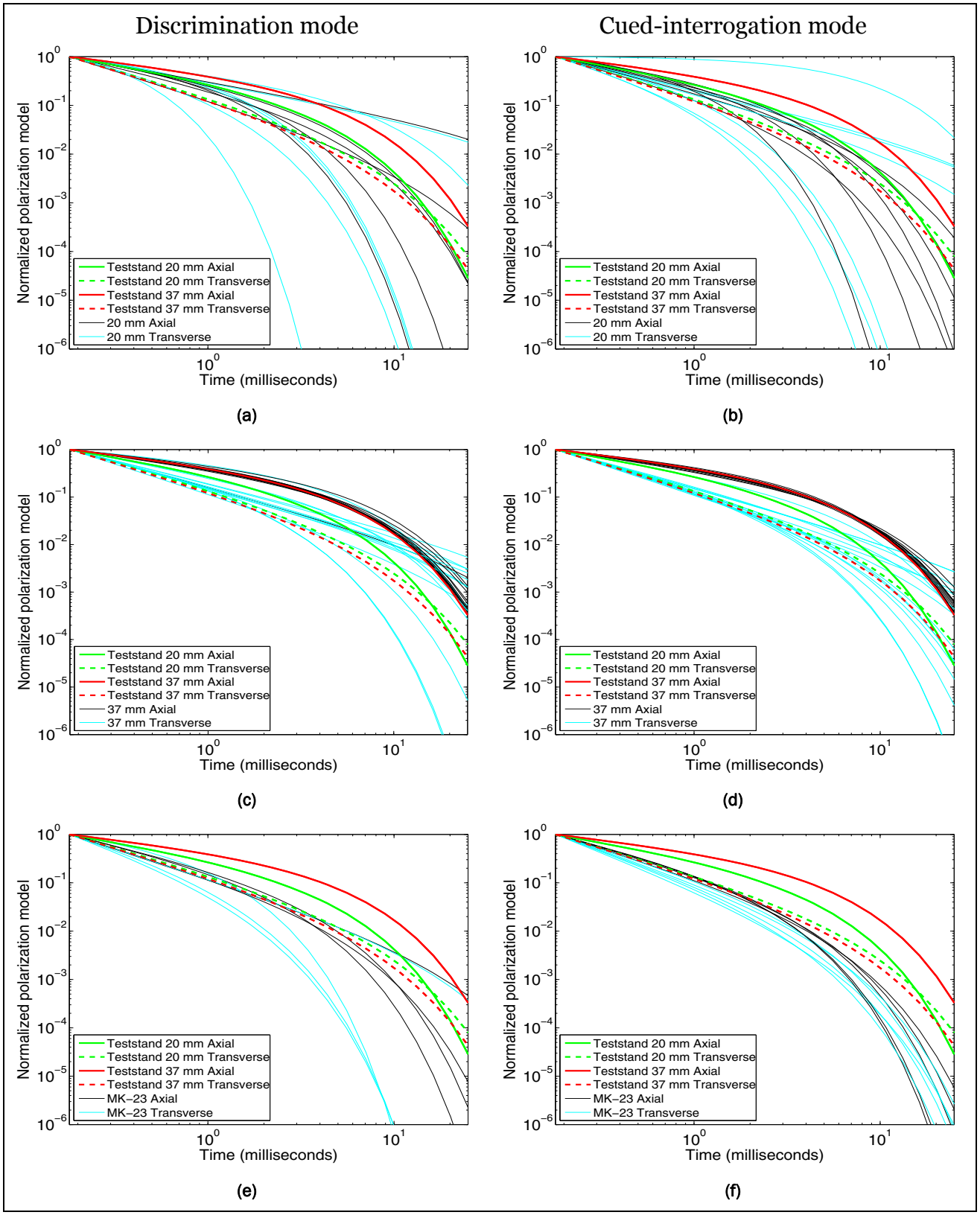


Figure 16. Normalized primary (axial) and secondary (transverse) polarization tensor models recovered over 20- and 37-mm projectiles and MK-23 practice bombs. The polarization curves were normalized by the value of the polarization at the first time channel.

# 4 Analysis of GEM-3 Cued Interrogation Data

## 4.1. GEM-3 data

The GEM-3 data were drift-corrected using the free-air calibration measurements that were collected before and after each anomaly was surveyed. The drift-corrected data still had a significant background shift due to the response of the soil in the vicinity of the detector head. This background appeared to be approximately constant over the 1-m by 1-m area of data collection. It was removed by fitting a linear polynomial to the points on the boundaries of the template, away from the influence of the item being measured. Figure 17 presents images of the data over a 50-caliber bullet and a 20-mm projectile and Figure 18 presents images of the data over two 37-mm projectiles. The magnitude of the data, the shape of the spatial anomaly, and the character of the frequency spectrum provide information that is diagnostic of the object's identity.

## 4.2. Inversion of GEM-3 data

The data over 58 GEM-3 anomalies were inverted using a three-dipole instantaneous polarization model (see Report 6). This involved finding the three real and imaginary components of the polarization tensor at each frequency, along with three Euler angles that define the orientation of the item as well as an estimated position and depth. Example inversion results over a 50-caliber bullet and a 37-mm projectile are given in Figures 19 and 20. For both items, the real and imaginary components of the model and data are in close agreement along a spatial profile and for the frequency spectrum directly over the estimated object location.

## 4.3. Analysis of feature vectors derived from GEM-3 data

The instantaneous amplitudes $L(\omega)$ of the three-dipole inversions were fit to the following four-parameter model of Miller et al. (2001)

$$L(\omega) = k\left(s + \frac{(i\omega\tau)^c - 2}{(i\omega\tau)^c + 1}\right) \tag{2}$$

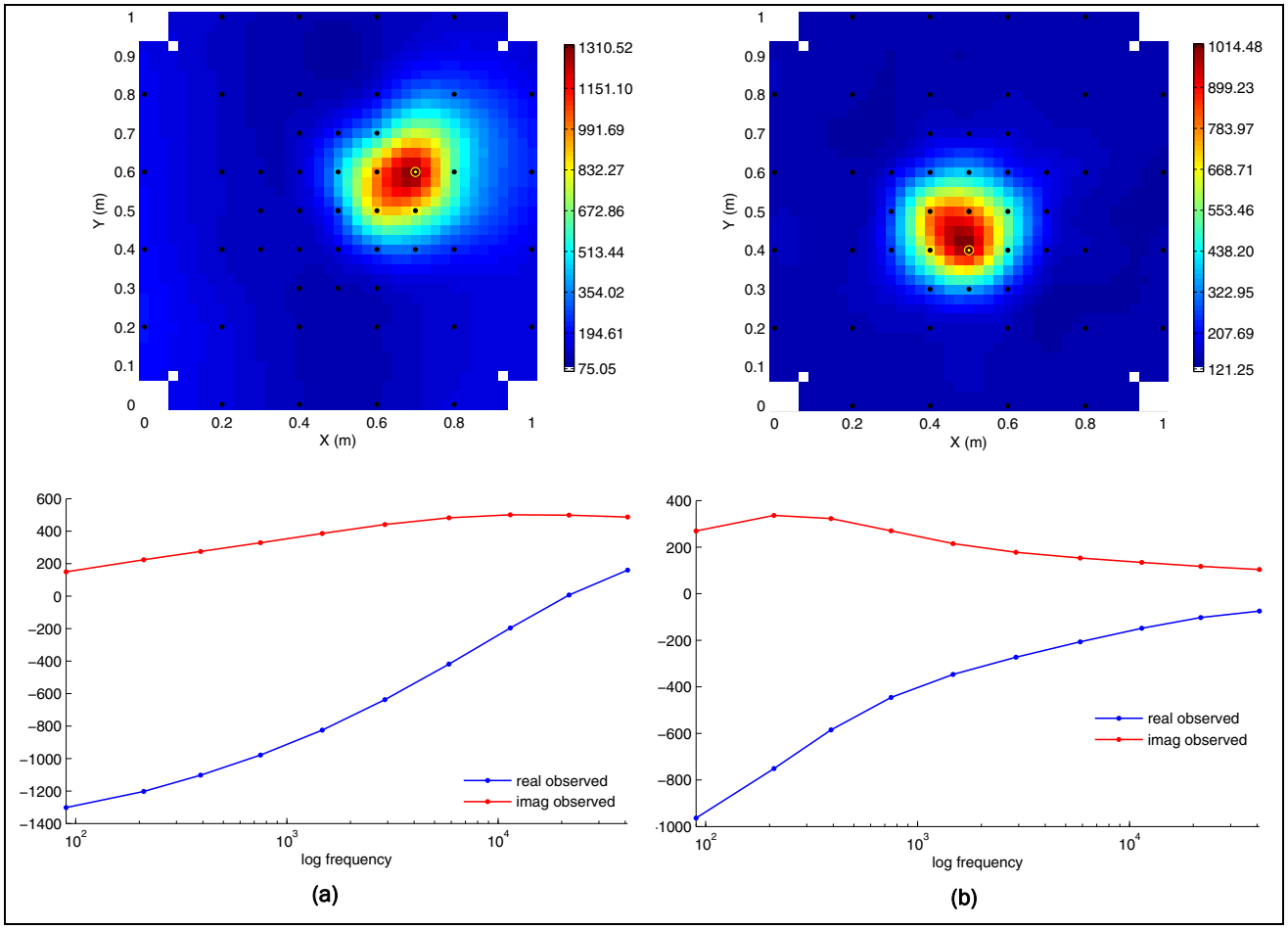


Figure 17. Images of GEM-3 cued-interrogation data over a 50-caliber bullet at the 2-cm depth (a) and a 20-mm projectile at the 7-cm depth (b). The plan view represents a gridded image of the absolute value at a frequency of 90 Hz with observation locations shown in black. The frequency spectrum is for points with maximum amplitude.

where:

$\omega$ = angular frequency
$k$ = object amplitude
$\tau$ = response time constant
$s$ = factor that controls the magnitude of asymptotes at high and low frequency
$c$ = parameter that controls the width of the in-phase peak response (Figure 21).

The parameter plots indicate that the amplitude and time-constant provide excellent separation between the hazardous 37-mm projectiles and the non-hazardous 50-caliber bullets and 20-mm projectiles. Some class separation is inherent in the $c$- and $s$-parameter plots, except there is partial overlap between the 20- and 37-mm parameter spreads.

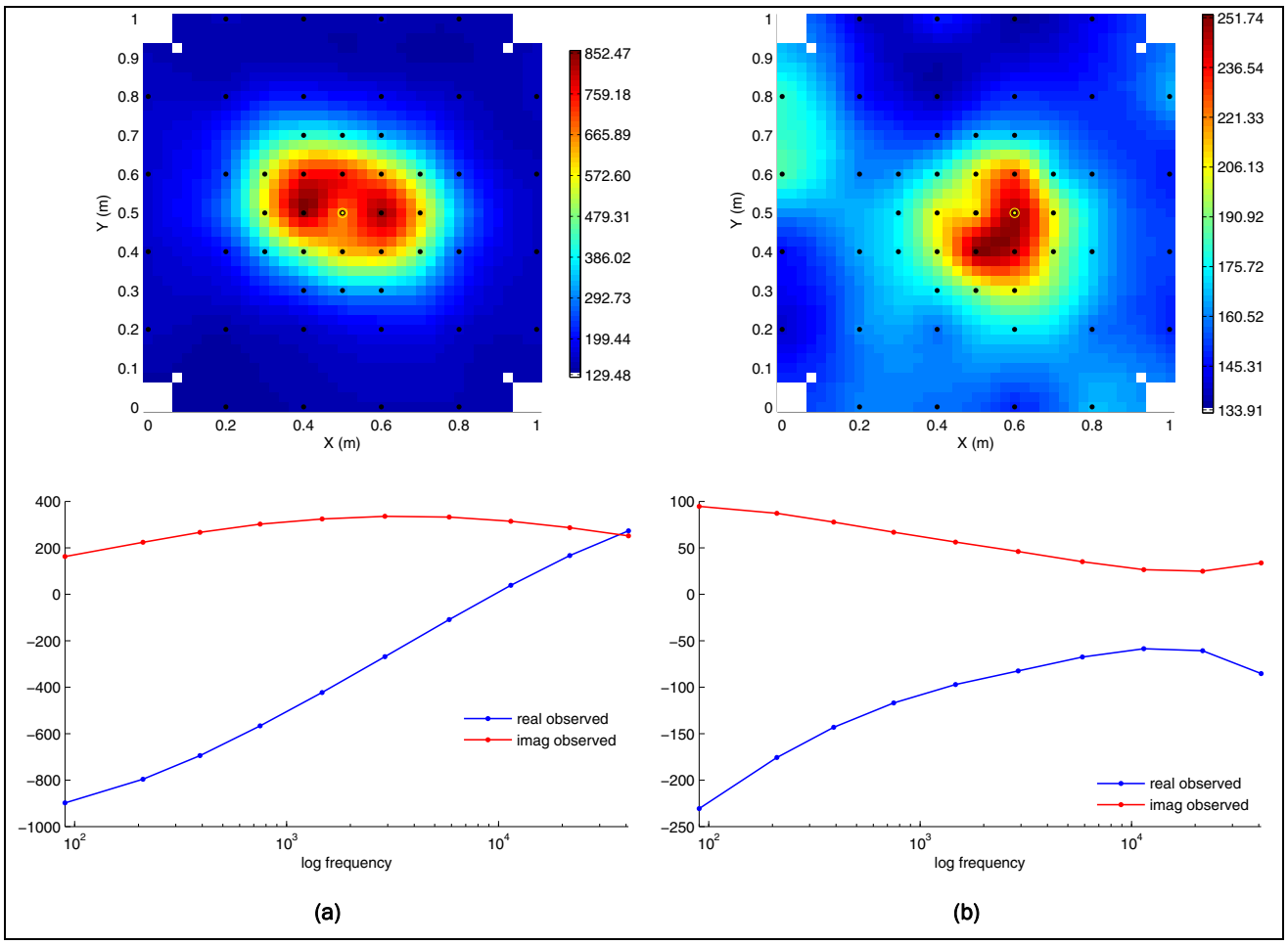


Figure 18. Images of GEM-3 cued-interrogation data over emplaced 37-mm projectiles at depths of 16 cm (a) and 28 cm (b). The plan view represents a gridded image of the absolute value at a frequency of 90 Hz, with observation locations shown in black. The frequency spectrum is for the point at (0.5 m E, 0.5 m N) for (a) and (0.6 m E, 0.5 m N) for (b).

The amplitude and time-constant features also provide excellent separation between the 50-caliber bullets and the 20-mm projectiles. Within the τ plot, the two 50-caliber bullets in the 20-mm cluster and the three 20-mm projectiles in the 50-caliber cluster most likely correspond to mislabeled items. All five items were found more than 50 cm from the location estimated from inversion of the GEM-3 data. Given the high density of items found at the site, it is quite likely that an alternate nearby item was mistakenly identified as the anomaly source. The five outliers in the τ plot are the same five outliers in the amplitude plot (the three lowest amplitude 20-mm projectiles and the two high amplitude, 50-caliber bullets).

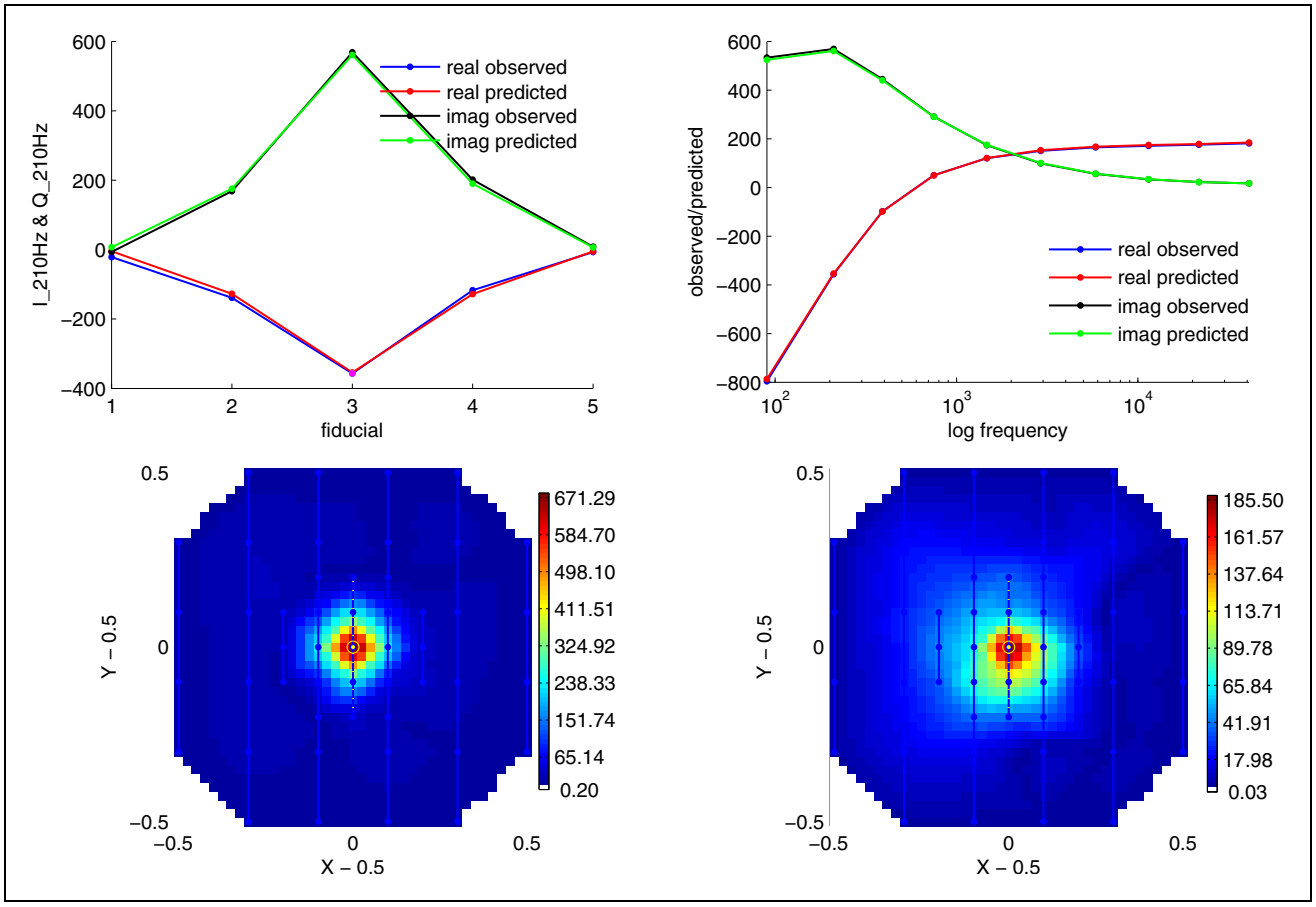


Figure 19. Example GEM-3 inversion over a 50-caliber bullet at the 5-cm depth. The top left view shows a spatial profile of the real and imaginary model and data at a frequency of 210 Hz, along the line directly over the center of the target. The top right view shows the modeled and measured frequency spectrum at the point with maximum amplitude (0 m E, 0 m N). The bottom left and right views are gridded representations of the real component of the data at frequencies of 210 and 21690 Hz, respectively.

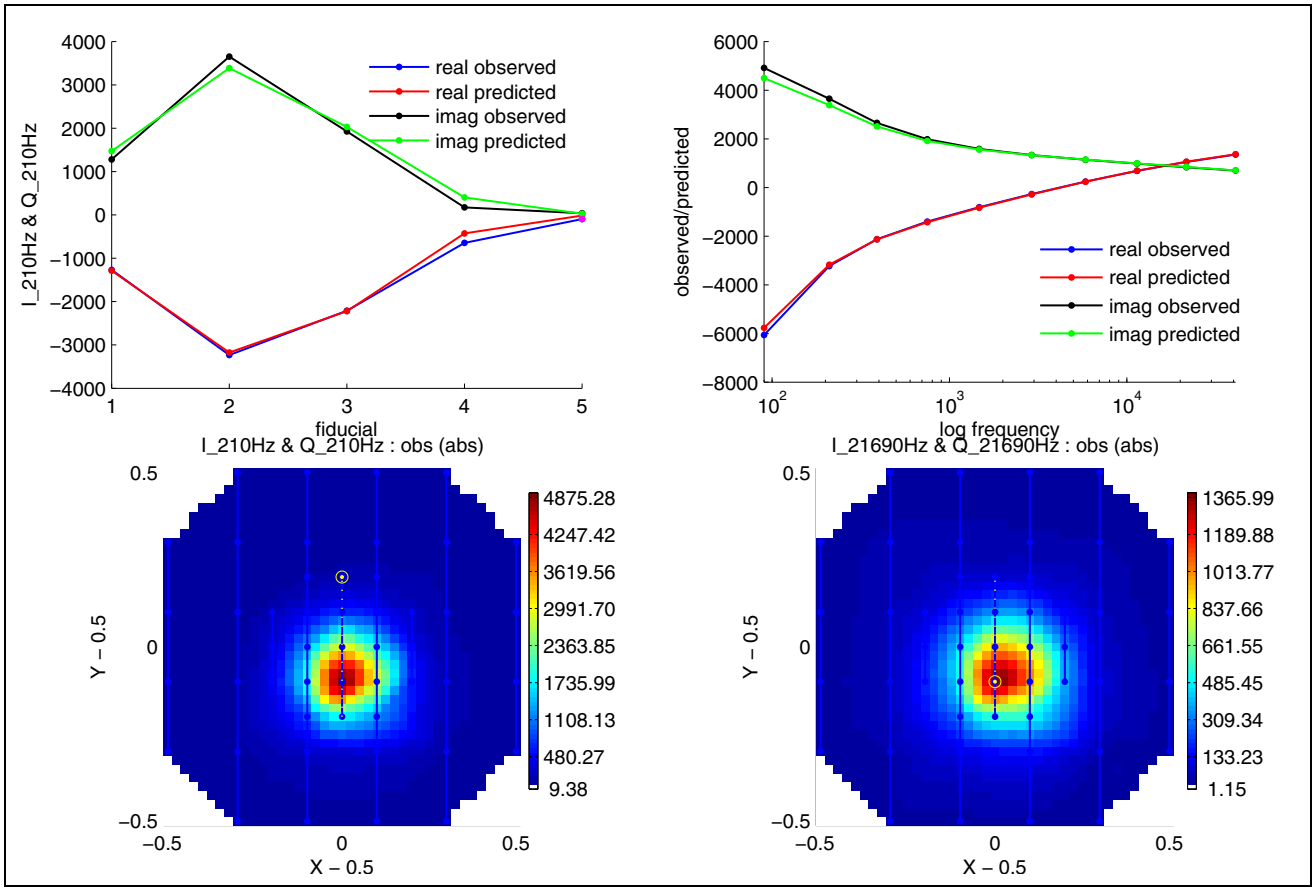


Figure 20. Example GEM-3 inversion over a 37-mm projectile at 10 cm. The top left view shows a spatial profile of the real and imaginary model and data at a frequency of 210 Hz, along the line directly over the center of the target. The top right view shows the modeled and measured frequency spectrum at the point with maximum amplitude. The bottom left and right views are gridded representations of the real component of the data at frequencies of 210 and 21,690 Hz, respectively.

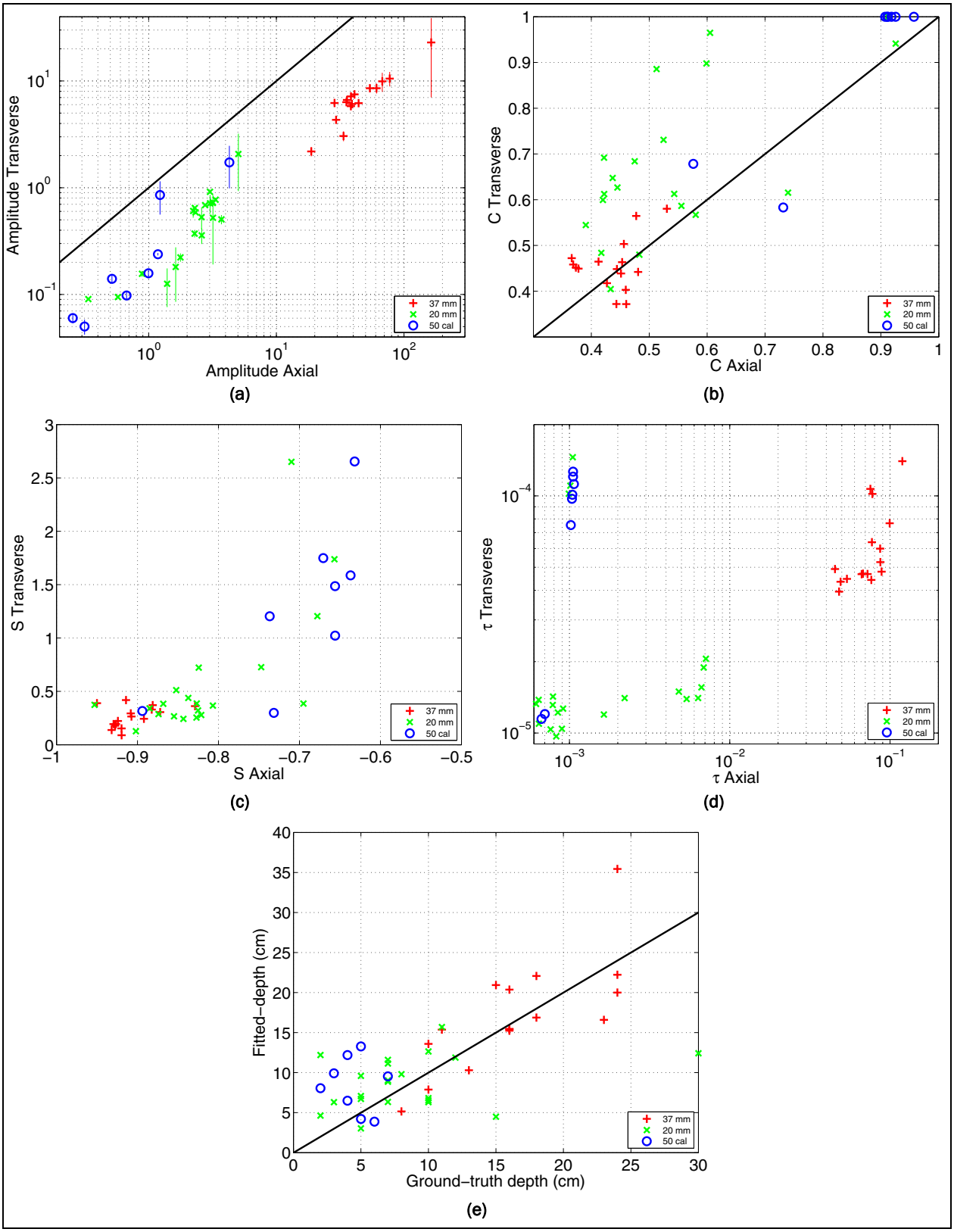


Figure 21. Polarization tensor parameter recovered from GEM-3 data collected at the 20-mm Range Fan: (a) amplitude of the Miller et al. (2001) model; (b) Miller c parameter; (c) Miller s parameter; (d) Miller time-constant parameter; and (e) actual versus predicted depth.

# 5 Discussion

One of the primary objectives of this report was to compare the discrimination potential of EM-63 data collected in discrimination and cued-interrogation modes. The higher quality, better positioning, and denser coverage of the cued-interrogation data result in a significant improvement in the discrimination potential of the system. This statement is best illustrated by Figures 12 and 14. The primary and secondary polarizations of the 37-mm projectiles and MK-23 practice bombs are more tightly clustered for the cued-interrogation data and agree closely with previously derived test-stand values (for the 37-mm projectiles). In addition, the secondary and tertiary polarizations are in close agreement for the 37-mm projectiles and MK-23 practice bombs, so that a feature related to the difference (or spread) in those polarizations has good discrimination potential. This is not the case for the discrimination mode data, where there are often large differences between the secondary and tertiary polarizations. Lastly, both methods return good estimates of the time-decay characteristics of the 37-mm projectiles and MK-23 practice bombs, with significant variations in recovered decays for the smaller 20-mm projectiles.

The following features provide useful discrimination information for both the 37-mm projectiles and MK-23 practice bombs.

- The size of the primary polarization (either $L_1(t_1)$ or the integrated polarization);
- The time decay (must be very fast for an MK-23);
- For the cued-interrogation mode data only, the difference between the secondary and tertiary polarizations;
- For the cued-interrogation mode data only, the ratio of the secondary to primary polarizations.

In summary,

- For the MK-23 practice bombs, a much richer set of feature vectors from the cued-interrogation mode data could be used, which could potentially significantly reduce false alarms over the discrimination mode data;

- For 37-mm projectiles, a size and a time-decay feature appear to be all that are required for good discrimination performance on 37-mm projectiles. Thus, only a marginal improvement in discrimination potential is expected when using cued-interrogation data.
- Neither method displayed any significant discrimination potential if the munition of concern was a 20-mm projectile.

For the GEM-3 data, which were collected in cued-interrogation mode, the amplitude and time constants of the four-parameter model of Miller et al. (2001) appeared to provide good discrimination potential. In particular:

- All 37-mm projectiles could be clearly distinguished from 50-caliber bullets and 20-mm projectiles;
- Except for five items (which are suspected to be mislabeled), the 50-caliber bullets and 20-mm projectiles were well separated in feature space.

Thus, when deployed in a cued-interrogation mode, the GEM-3 appears to be capable of distinguishing 37-mm projectiles from 20-mm projectiles AND of distinguishing 20-mm projectiles from 50-caliber bullets. While this result is extremely promising, it should be kept in mind that the data collection process required a template and was relatively slow. To provide a practical solution to this small object discrimination problem, much faster data collection rates need to be achieved.

# References

Billings, S. D., L. R. Pasion, L. Beran, D. Oldenburg, D. Sinex, L. Song, and N. Lhomme. 2007. *Demonstration report for the Former Lowry Bombing and Gunnery Range, ESTCP MM-0504: Practical discrimination strategies for application to live sites*.

Miller, J. T., T. H. Bell, J. Soukup, and D. Keiswetter. 2001. Simple phenomenological models for wide-band frequency domain electromagnetic induction. In *IEEE Transactions on Geoscience and Remote Sensing* 39:1294–1298.

Pasion, L. P., and D. Oldenburg. 2001. A discrimination algorithm for UXO using time domain electromagnetics. *Journal of Engineering and Environmental Geophysics* 28:91–102.

# Appendix A: Pasion-Oldenburg Three-Dipole Fits to Cued and Discrimination Mode Anomalies

The images on the following pages summarize the inversion fits for discrimination and cued-interrogation data collected at the Rocket Range and the 20-mm Range Fan. The item listed as cell 3 corresponds to the anomaly over an MK-23 practice bomb, while the item listed as cell 418 corresponds to a 37-mm projectile. In both cases, the discrimination mode data appear first, followed by the cued-interrogation data.

Key for interpreting the images in the appendix:

- The three columns and four rows of images comprise plan views of the data, model, and residuals (from left to right) and four different time channels: 1, 7, 14, and 21 (from top to bottom);
- To the right of the images are four profiles of observed and predicted data (in time channels 1, 7, 14, and 21), along the red line marked in the adjacent images;
- The table at top right shows the three components of the polarizability tensor at the 26 time channels measured by the EM-63;
- The plot at center right shows the observed and predicted sounding at anomaly maximum, along with the estimated noise floor;
- The plot at bottom right shows the three components of the polarizability matrix as a function of time;
- The table immediately below the images shows the parameters (middle row) and estimated uncertainties (bottom row) of the recovered model;
- The table at the very bottom of the page presents the technical details of the inversion.

# 1 Cell 3 ()

Fit? None Comment Save Fits

Contents

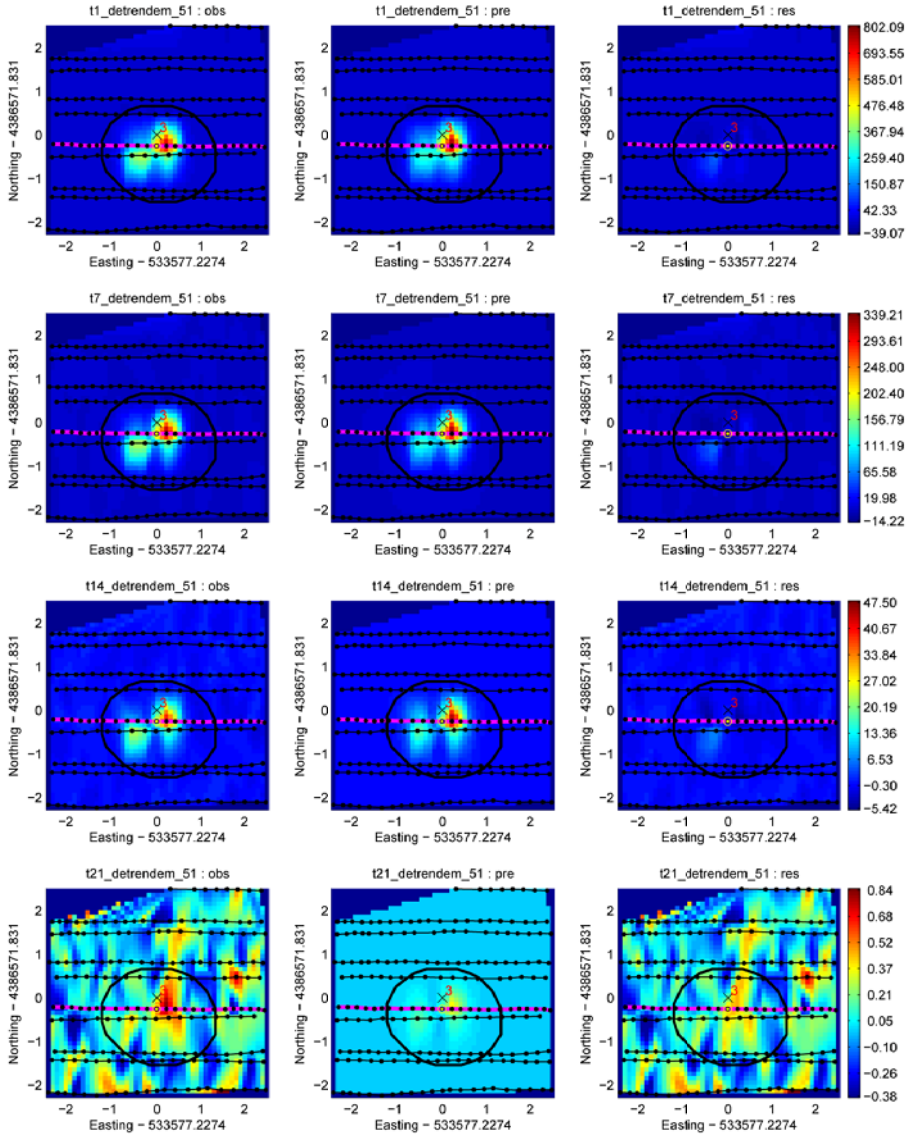


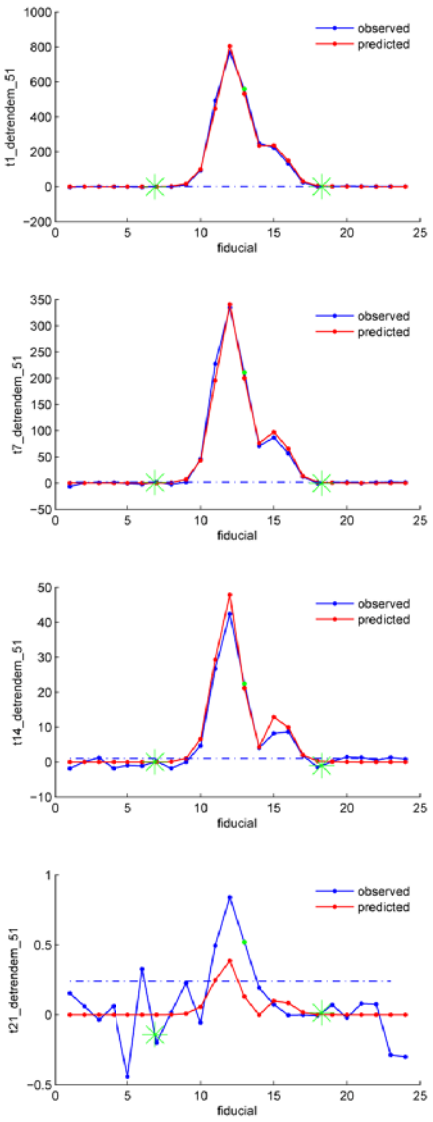


| t(ms) | $L_x$ | $L_y$ | $L_z$ |
|---|---|---|---|
| 0.18 | 66.413 | 0.036725 | 9.5407 |
| 0.195 | 61.439 | 0.03414 | 8.6024 |
| 0.22 | 54.5772 | 0.03051 | 7.3437 |
| 0.25 | 48.0621 | 0.026989 | 6.1905 |
| 0.29 | 41.368 | 0.023287 | 5.053 |
| 0.34 | 35.1095 | 0.01974 | 4.0386 |
| 0.405 | 29.1785 | 0.016296 | 3.1279 |
| 0.485 | 23.9687 | 0.013201 | 2.3755 |
| 0.59 | 19.1938 | 0.010313 | 1.7327 |
| 0.72 | 15.1512 | 0.0078395 | 1.2311 |
| 0.89 | 11.6081 | 0.0056729 | 0.83142 |
| 1.105 | 8.6765 | 0.0039121 | 0.53633 |
| 1.375 | 6.31 | 0.0025494 | 0.32828 |
| 1.725 | 4.3905 | 0.0015248 | 0.18514 |
| 2.17 | 2.9166 | 0.00082772 | 0.095489 |
| 2.74 | 1.8227 | 0.00039551 | 0.043777 |
| 3.465 | 1.0589 | 0.0001617 | 0.017403 |
| 4.385 | 0.56178 | 5.4376e-005 | 0.0057903 |
| 5.565 | 0.26363 | 1.4074e-005 | 0.0015163 |
| 7.07 | 0.10636 | 2.6308e-006 | 0.00029518 |
| 8.905 | 0.037122 | 3.5587e-007 | 4.299e-005 |
| 10.78 | 0.013174 | 4.7602e-008 | 6.3126e-006 |
| 13.22 | 0.0035596 | 3.5871e-009 | 5.467e-007 |
| 16.28 | 0.00071949 | 1.4506e-010 | 2.6828e-008 |
| 20.15 | 9.9563e-005 | 2.602e-012 | 6.2703e-010 |
| 25.14 | 8.1521e-006 | 1.5157e-014 | 5.2492e-012 |

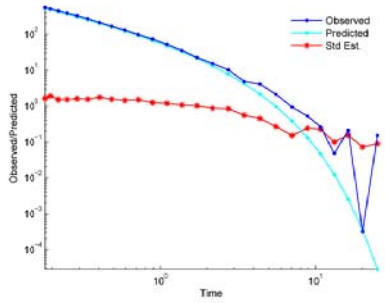


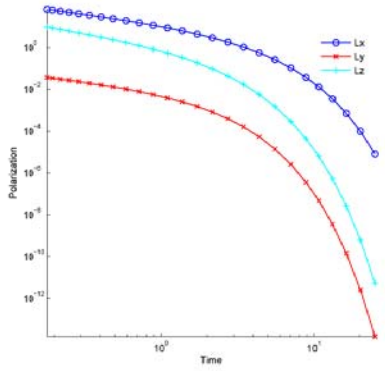


| Easting | Northing | Depth | $\theta$ | $\phi$ | $\delta$ | $\kappa_1$ | $\beta_1$ | $\gamma_1$ | $\kappa_2$ | $\beta_2$ | $\gamma_2$ | $\kappa_3$ | $\beta_3$ | $\gamma_3$ | misfit | CorrCoef |
|---|---|---|---|---|---|---|---|---|---|---|---|---|---|---|---|---|
| 533577.1571 | 4386571.581 | -0.097778 | -84.8103 | 23.2977 | 52.6892 | 1.6376 | 1.1231 | 1.1005 | 15.7972 | 0.88597 | 2.1635 | 0.012684 | 0.72482 | 1.001 | 1.2741 | 0.95501 |
| ±0.0014463 | ± 0 | ±0.0023929 | ± 1.3422 | ± 0.58676 | ± 1.2286 | ± 0.031901 | ± 0.01951 | ± 0.029649 | ± 0.27378 | ± 0.010881 | ± 0.050584 | ± 0.01389 | ± 0.98042 | ± 0 | | |

| firstorderopt | iterations | funcCount | cgiterations | algorithm | message | numstartmodels | time | S2N |
|---|---|---|---|---|---|---|---|---|
| 18514.3731 | 21 | 352 | 111 | large-scale: trust-region reflective Newton | Maximum number of iterations exceeded; increase options.MaxIter | 7 | 41.0949 | 20 of 26 channels/freqs inverted. Minimum S2N = 2.00 |

# 1 Cell 3 ($I12_1$)

Fit? None Comment Save Fits

Contents

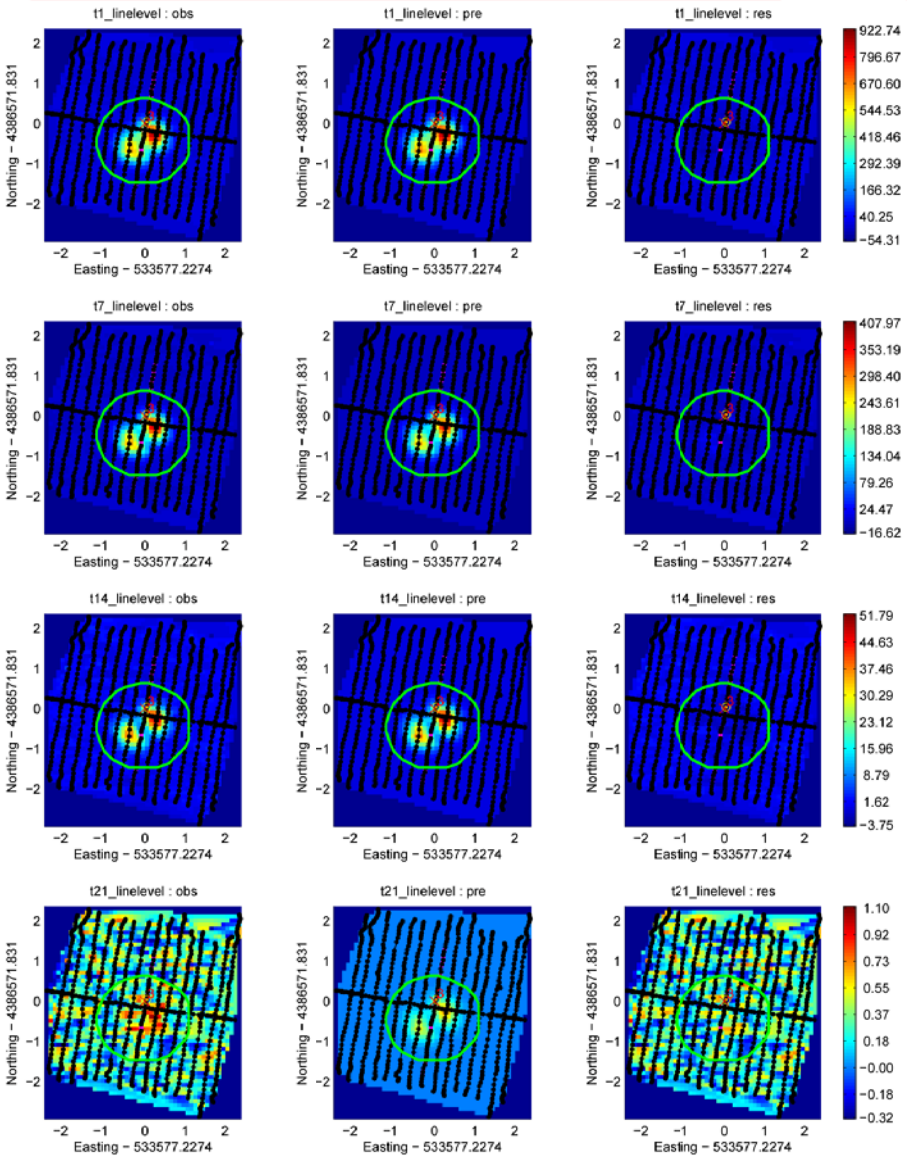


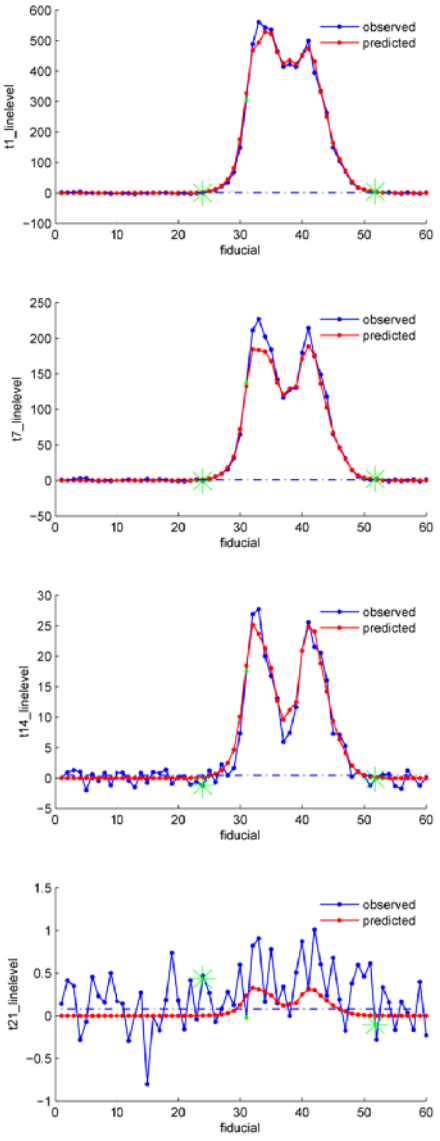


| t(ms) | $L_x$ | $L_y$ | $L_z$ |
|---|---|---|---|
| 0.18 | 60.0019 | 6.7114 | 5.7977 |
| 0.195 | 55.1286 | 5.9296 | 5.2913 |
| 0.22 | 48.478 | 4.9169 | 4.5993 |
| 0.25 | 42.2478 | 4.0282 | 3.9507 |
| 0.29 | 35.9418 | 3.1915 | 3.2943 |
| 0.34 | 30.1436 | 2.4822 | 2.6922 |
| 0.405 | 24.7474 | 1.8778 | 2.1348 |
| 0.485 | 20.097 | 1.4038 | 1.6591 |
| 0.59 | 15.9188 | 1.0184 | 1.2389 |
| 0.72 | 12.4523 | 0.73054 | 0.89954 |
| 0.89 | 9.4744 | 0.50876 | 0.61989 |
| 1.105 | 7.0568 | 0.34789 | 0.40666 |
| 1.375 | 5.1372 | 0.23373 | 0.25197 |
| 1.725 | 3.5998 | 0.15193 | 0.143 |
| 2.17 | 2.4274 | 0.095964 | 0.073608 |
| 2.74 | 1.5559 | 0.05835 | 0.033319 |
| 3.465 | 0.93945 | 0.034002 | 0.012897 |
| 4.385 | 0.52674 | 0.018815 | 0.0041052 |
| 5.565 | 0.26708 | 0.0096908 | 0.0010048 |
| 7.07 | 0.11971 | 0.0045801 | 0.00017751 |
| 8.905 | 0.047803 | 0.0020128 | 2.2732e-005 |
| 10.78 | 0.019554 | 0.000929 | 2.9048e-006 |
| 13.22 | 0.0063855 | 0.00036316 | 2.0838e-007 |
| 16.28 | 0.0016448 | 0.00012011 | 8.0095e-009 |
| 20.15 | 0.00031084 | 3.1946e-005 | 1.363e-010 |
| 25.14 | 3.825e-005 | 6.2775e-006 | 7.5099e-013 |

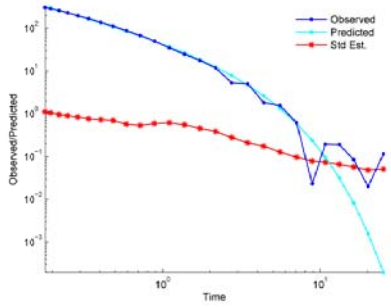


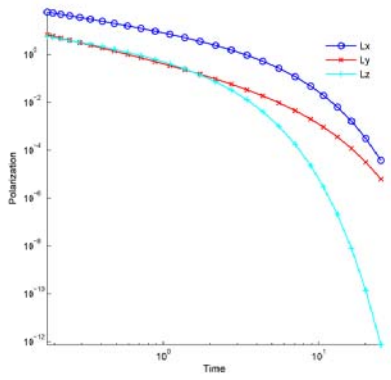


| Easting | Northing | Depth | $\theta$ | $\phi$ | $\delta$ | $\kappa_1$ | $\beta_1$ | $\gamma_1$ | $\kappa_2$ | $\beta_2$ | $\gamma_2$ | $\kappa_3$ | $\beta_3$ | $\gamma_3$ | misfit | CorrCoef |
|---|---|---|---|---|---|---|---|---|---|---|---|---|---|---|---|---|
| 533577.1752 | 4386571.4188 | -0.041316 | 58.7471 | 96.7824 | -84.9429 | 1.3506 | 0.95459 | 1 | 11.801 | 0.98781 | 2.6591 | 0.53829 | 1.4987 | 3.8518 | 5.0111 | 0.83852 |
| ±0.00044509 | ±0.00039806 | ±0.00075687 | ± 0.22302 | ± 2.3929 | ± 0.072031 | ± 0.035218 | ± 0.021747 | ± 0 | ± 0.10775 | ± 0.0055687 | ± 0.033953 | ± 0.0077894 | ± 0 | ± 0.24357 | | |

| firstorderopt | iterations | funcCount | cgiterations | algorithm | message | numstartmodels | time | S2N |
|---|---|---|---|---|---|---|---|---|
| 91267.078 | 21 | 352 | 95 | large-scale: trust-region reflective Newton | Maximum number of iterations exceeded; increase options.MaxIter | 5 | 32.5771 | 26 of 26 channels/freqs inverted. Minimum S2N = 2.00 |

# 1 Cell 418 ()

Fit? None Comment Save Fits

Contents

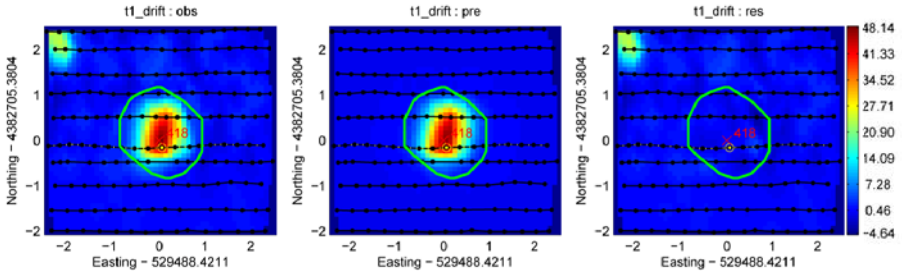


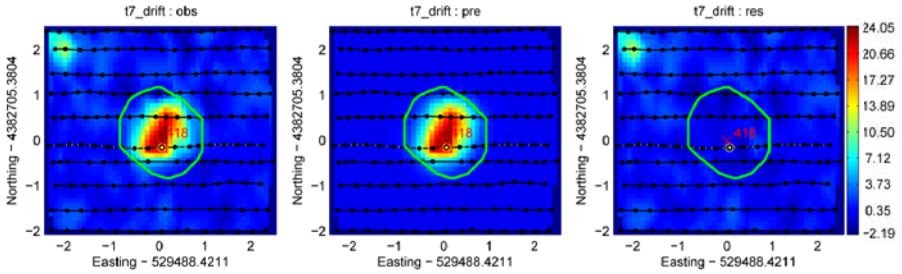


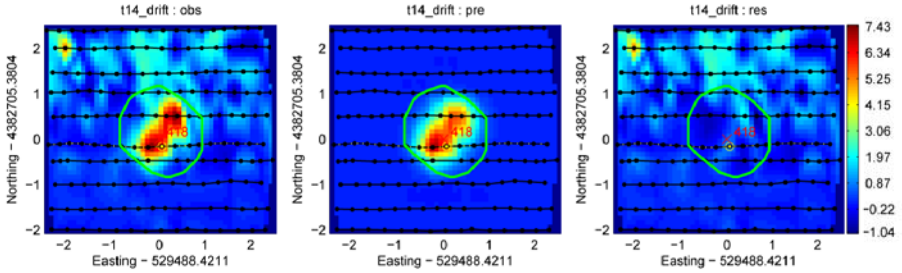


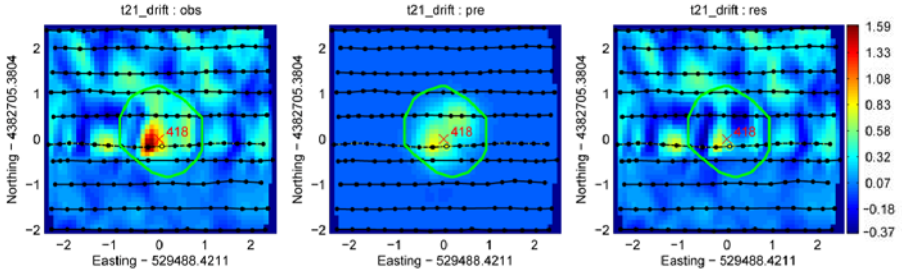


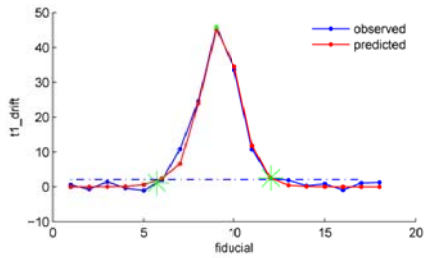


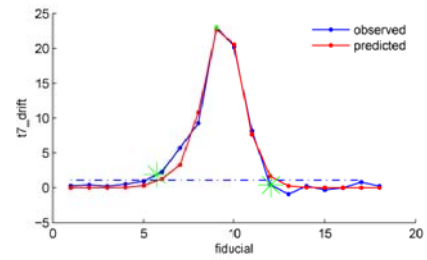


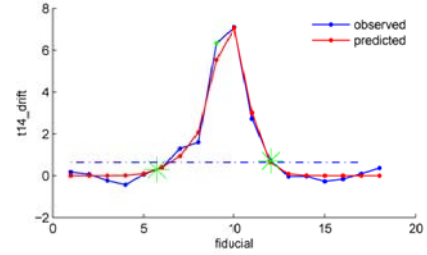


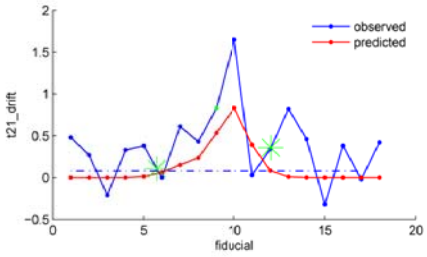


| t(ms) | $L_x$ | $L_y$ | $L_z$ |
|---|---|---|---|
| 0.18 | 4.9804 | 4.8956 | 7.9426 |
| 0.195 | 4.6113 | 4.5356 | 7.6235 |
| 0.22 | 4.1058 | 4.0371 | 7.1636 |
| 0.25 | 3.6302 | 3.5615 | 6.7024 |
| 0.29 | 3.1464 | 3.0703 | 6.1983 |
| 0.34 | 2.6988 | 2.6085 | 5.6929 |
| 0.405 | 2.2793 | 2.1683 | 5.1754 |
| 0.485 | 1.9146 | 1.7793 | 4.6805 |
| 0.59 | 1.5834 | 1.4209 | 4.1827 |
| 0.72 | 1.305 | 1.116 | 3.7157 |
| 0.89 | 1.0614 | 0.84794 | 3.2575 |
| 1.105 | 0.85896 | 0.62602 | 2.8272 |
| 1.375 | 0.69286 | 0.44741 | 2.4275 |
| 1.725 | 0.55363 | 0.30374 | 2.047 |
| 2.17 | 0.44039 | 0.19515 | 1.6952 |
| 2.74 | 0.34819 | 0.11659 | 1.3707 |
| 3.465 | 0.27404 | 0.063828 | 1.0777 |
| 4.385 | 0.21469 | 0.031334 | 0.81827 |
| 5.565 | 0.16687 | 0.01328 | 0.59263 |
| 7.07 | 0.12873 | 0.0046943 | 0.40506 |
| 8.905 | 0.099474 | 0.0013914 | 0.26226 |
| 10.78 | 0.079781 | 0.0004172 | 0.17184 |
| 13.22 | 0.062486 | 9.0378e-005 | 0.10127 |
| 16.28 | 0.048145 | 1.3823e-005 | 0.053385 |
| 20.15 | 0.036322 | 1.342e-006 | 0.024331 |
| 25.14 | 0.026592 | 6.9439e-008 | 0.0090639 |

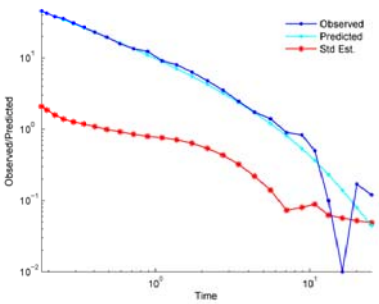


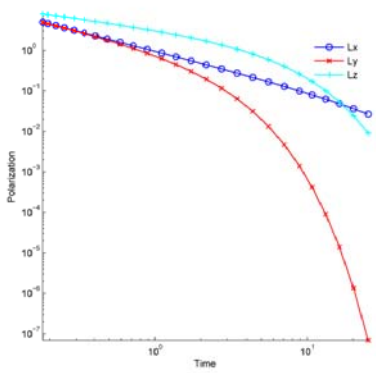


| Easting | Northing | Depth | $\theta$ | $\phi$ | $\delta$ | $\kappa_1$ | $\beta_1$ | $\gamma_1$ | $\kappa_2$ | $\beta_2$ | $\gamma_2$ | $\kappa_3$ | $\beta_3$ | $\gamma_3$ | misfit | CorrCoef |
|---|---|---|---|---|---|---|---|---|---|---|---|---|---|---|---|---|
| 529488.5128 | 4382705.5414 | -0.22 | -44.9795 | 90.4643 | 90 | 3.605 | 0.47919 | 5.6613 | 0.96634 | 0.95834 | 50 | 1.2594 | 0.85009 | 1.7993 | 1.9951 | 0.82023 |
| ±0.0042723 | ±0.0042198 | ± 0 | ± 1.8781 | ± 0.61112 | ± 0 | ± 0.13645 | ± 0.031641 | ± 0.43429 | ± 0.040721 | ± 0.029487 | ± 0 | ± 0.49887 | ± 0.23533 | ± 1.0828 | | |

| firstorderopt | iterations | funcCount | cgiterations | algorithm | message | numstartmodels | time | S2N |
|---|---|---|---|---|---|---|---|---|
| 1747.7903 | 24 | 400 | 119 | large-scale: trust-region reflective Newton | Optimization terminated: relative function value changing by less than OPTIONS.TolFun. | 10 | 55.2502 | 26 of 26 channels/freqs inverted. Minimum S2N = 2.00 |

# 1 Cell 418 ($21_14_418$)

Fit? None Comment Save Fits

Contents

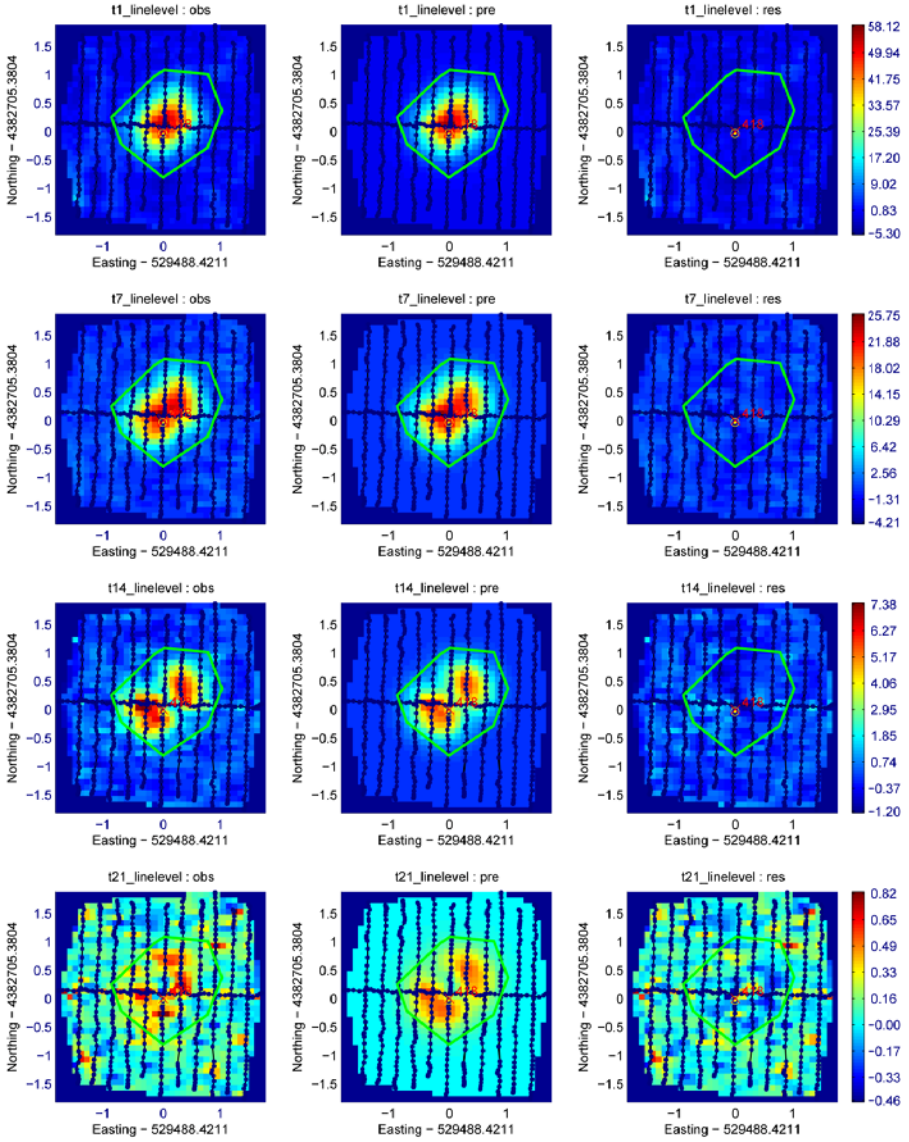


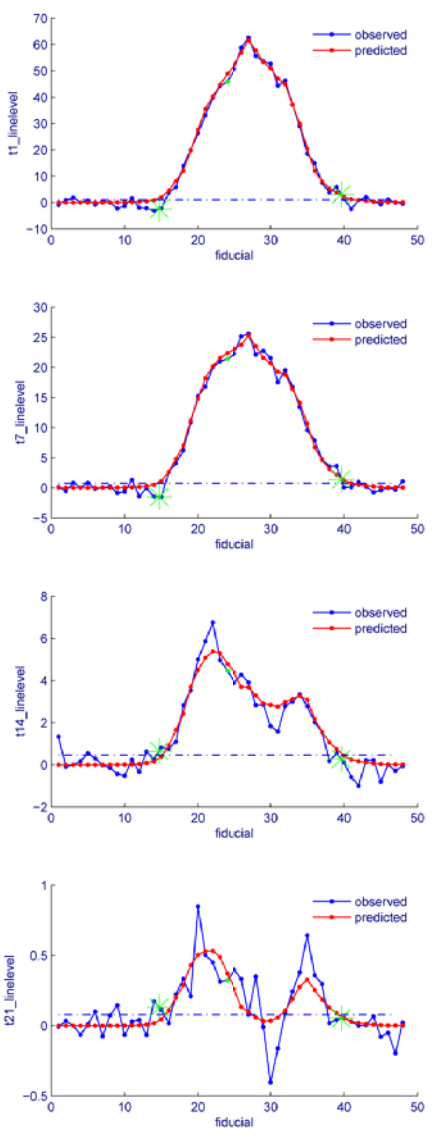


| t(ms) | $L_x$ | $L_y$ | $L_z$ |
|---|---|---|---|
| 0.18 | 4.6936 | 10.4096 | 4.9403 |
| 0.195 | 4.3403 | 9.976 | 4.5318 |
| 0.22 | 3.8573 | 9.3521 | 3.9751 |
| 0.25 | 3.4037 | 8.7273 | 3.4545 |
| 0.29 | 2.9432 | 8.0458 | 2.9284 |
| 0.34 | 2.5183 | 7.3639 | 2.4458 |
| 0.405 | 2.121 | 6.6671 | 1.9979 |
| 0.485 | 1.7766 | 6.0025 | 1.613 |
| 0.59 | 1.4648 | 5.3357 | 1.2684 |
| 0.72 | 1.2034 | 4.712 | 0.98378 |
| 0.89 | 0.97562 | 4.1021 | 0.74061 |
| 1.105 | 0.78683 | 3.5316 | 0.54457 |
| 1.375 | 0.6325 | 3.004 | 0.3903 |
| 1.725 | 0.5036 | 2.5046 | 0.26818 |
| 2.17 | 0.39915 | 2.0464 | 0.17649 |
| 2.74 | 0.31442 | 1.6278 | 0.10973 |
| 3.465 | 0.24654 | 1.2546 | 0.063773 |
| 4.385 | 0.19243 | 0.92973 | 0.034089 |
| 5.565 | 0.149 | 0.65329 | 0.016269 |
| 7.07 | 0.1145 | 0.43004 | 0.0067549 |
| 8.905 | 0.088147 | 0.2662 | 0.0024585 |
| 10.78 | 0.070475 | 0.1667 | 0.00091523 |
| 13.22 | 0.055012 | 0.092687 | 0.0002645 |
| 16.28 | 0.042238 | 0.045451 | 5.8481e-005 |
| 20.15 | 0.031751 | 0.018919 | 9.1163e-006 |
| 25.14 | 0.023156 | 0.0062751 | 8.7561e-007 |

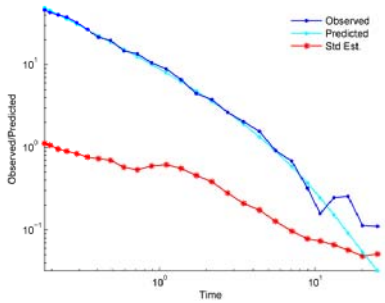


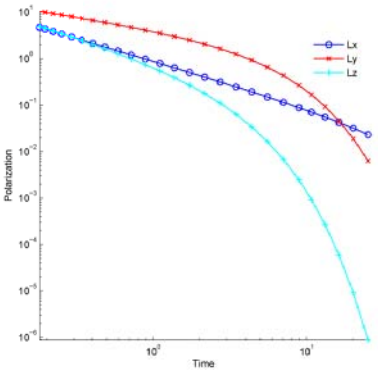


| Easting | Northing | Depth | $\theta$ | $\phi$ | $\delta$ | $\kappa_1$ | $\beta_1$ | $\gamma_1$ | $\kappa_2$ | $\beta_2$ | $\gamma_2$ | $\kappa_3$ | $\beta_3$ | $\gamma_3$ | misfit | CorrCoef |
|---|---|---|---|---|---|---|---|---|---|---|---|---|---|---|---|---|
| 529488.4991 | 4382705.5677 | -0.25987 | 39.0375 | 9.5008 | 11.8777 | 0.96255 | 0.99845 | 2.3516 | 0.88665 | 0.97395 | 49.807 | 4.624 | 0.49413 | 5.0188 | 3.0158 | 0.79074 |
| ±0.0019236 | ±0.0019446 | ± 0.015443 | ± 2.6804 | ± 2.0991 | ± 2.646 | ± 0.19411 | ± 0.061362 | ± 0.43461 | ± 0.078836 | ± 0.028523 | ± 3.3165 | ± 0.41029 | ± 0.012443 | ± 0.16553 | | |

| firstorderopt | iterations | funcCount | cgiterations | algorithm | message | numstartmodels | time | S2N |
|---|---|---|---|---|---|---|---|---|
| 37146.0122 | 21 | 352 | 147 | large-scale: trust-region reflective Newton | Optimization terminated: relative function value changing by less than OPTIONS.TolFun. | 5 | 46.488 | 26 of 26 channels/freqs inverted. Minimum S2N = 2.00 |

# REPORT DOCUMENTATION PAGE

*Form Approved*
*OMB No. 0704-0188*



| 1. REPORT DATE *(DD-MM-YYYY)* | 2. REPORT TYPE | 3. DATES COVERED *(From - To)* |
|---|---|---|
| September 2008 | Report 9 of 9 | |

**4. TITLE AND SUBTITLE**

UXO Characterization: Comparing Cued Surveying to Standard Detection and Discrimination Approaches: Report 9 of 9 – Former Lowry Bombing and Gunnery Range; Comparison of UXO Characterization Performance Using Area and Cued-interrogation Survey Modes

**5a. CONTRACT NUMBER**
W912HZ-04-C-0039

**5b. GRANT NUMBER**

**5c. PROGRAM ELEMENT NUMBER**

**6. AUTHOR(S)**

Stephen D. Billings, Leonard R. Pasion, Kevin Kingdon, Sean Walker, and Jon Jacobson

**5d. PROJECT NUMBER**

**5e. TASK NUMBER**

**5f. WORK UNIT NUMBER**

**7. PERFORMING ORGANIZATION NAME(S) AND ADDRESS(ES)**

Sky Research, Inc.
445 Dead Indian Memorial Rd.
Ashland, OR 97520

**8. PERFORMING ORGANIZATION REPORT NUMBER**
ERDC/EL TR-08-40

**9. SPONSORING / MONITORING AGENCY NAME(S) AND ADDRESS(ES)**

Headquarters, U.S. Army Corps of Engineers
Washington, DC 20314-1000
U.S. Army Engineer Research and Development Center
Environmental Laboratory
3909 Halls Ferry Road
Vicksburg, MS 39180-6199

**10. SPONSOR/MONITOR'S ACRONYM(S)**

**11. SPONSOR/MONITOR'S REPORT NUMBER(S)**

**12. DISTRIBUTION / AVAILABILITY STATEMENT**

Approved for public release; distribution is unlimited.

**13. SUPPLEMENTARY NOTES**

**14. ABSTRACT**

This report describes the collection, processing, interpretation, and analysis of Geonics EM-63 and Geophex GEM-3 data collected in a cued-interrogation mode at the FLBGR and compares the discrimination potential of data collected in discrimination versus cued-interrogation modes. The higher quality, better positioning, and denser coverage of the EM-63 cued-interrogation data (compared to discrimination mode data) result in a significant improvement in the discrimination potential of the system. For the GEM-3 data, which were collected in cued-interrogation mode, the amplitude and time constants of the four-parameter model of Miller et al. appeared to provide good discrimination potential. When deployed in a cued-interrogation mode, the GEM-3 appears to be capable of distinguishing 37-mm projectiles from 20-mm projectiles and of distinguishing 20-mm projectiles from 50-caliber bullets.

**15. SUBJECT TERMS**

EMI sensors
Frequency-domain electromagnetic induction (FEM)
Ground penetrating radar
Time-domain electromagnetic induction (TEM)
Total-field magnetics
Unexploded ordnance (UXO)
UXO discrimination

| 16. SECURITY CLASSIFICATION OF: | | | 17. LIMITATION OF ABSTRACT | 18. NUMBER OF PAGES | 19a. NAME OF RESPONSIBLE PERSON |
|---|---|---|---|---|---|
| a. REPORT | b. ABSTRACT | c. THIS PAGE | | | 19b. TELEPHONE NUMBER *(include area code)* |
| UNCLASSIFIED | UNCLASSIFIED | UNCLASSIFIED | | 55 | |